An Acad Bras Cienc (2021) 93(Suppl. 2): e20201239 DOI 10.1590/0001-3765202120201239
Anais da Academia Brasileira de Ciências | *Annals of the Brazilian Academy of Sciences*
Printed ISSN 0001-3765 I Online ISSN 1678-2690
www.scielo.br/aabc | www.fb.com/aabcjournal

PALEONTOLOGY

Intraspecific variation in the axial skeleton of *Aetosauroides scagliai* (Archosauria: Aetosauria) and its implications for the aetosaur diversity of the Late Triassic of Brazil

VOLTAIRE D. PAES-NETO, JULIA BRENDA DESOJO, ANA CAROLINA B. BRUST, CESAR LEANDRO SCHULTZ, ÁTILA AUGUSTO S. DA-ROSA & MARINA B. SOARES

Abstract: Aetosauria represents a remarkable clade of armored pseudosuchians in which some of its oldest members are recovered from late Carnian units of Brazil. Three species are known: the mid-sized aetosaur *Aetosauroides scagliai*, which also occurs in Argentina, and two small-sized species, *Aetobarbakinoides brasiliensis* and *Polesinesuchus aurelioi*. We provide a detailed description and comparative analysis of the axial skeleton of *Aetosauroides*, identifying some diagnostic features as variable. These include the deep pocket pit lateral to the base of the neural spine, the presence of the infradiapophyseal laminae and the lateral fossa ventral to the neurocentral suture. These features are not found in smaller and immature *Aetosauroides* specimens, resembling the condition found in *Polesinesuchus*, which is based solely on a juvenile individual, as revealed by osteoderm microstructure analysis. As *Polesinesuchus* cannot be anatomically differentiated from other small individuals of *Aetosauroides*, we propose it as a junior synonym of *Aetosauroides scagliai*. Our results shrink the number of putative 'dwarf' aetosaurs, indicating that morphological variation related to ontogeny affects aetosaur taxonomy and phylogeny.

Key words: Pseudosuchia, growth series, juvenile, ontogeny, Osteohistology.

INTRODUCTION

The ontogeny of early Mesozoic archosaurs is still poorly understood, and little is known about morphological variation related to growth in extinct pseudosuchians (e.g. Ezcurra & Butler 2015, Nesbitt et al. 2018, Griffin et al. 2020). Aetosaurs represent a Late Triassic clade of diverse and abundant quadrupedal pseudosuchians, characterized by a small triangular skull and four rows of osteoderms covering the entire dorsal portion of the body (e.g. Desojo et al. 2013). Although they are generally mid-sized to large animals, reaching up to six meters of total length (Walker 1961, Parker 2008, Heckert et al. 2010, Desojo et al. 2013, Taborda et al. 2013), several species are considered small (Heckert & Lucas 1999, Schoch 2007, Parker et al. 2008, Desojo et al. 2012, 2013, Small & Martz 2013, Roberto-da-Silva et al. 2014, Heckert et al. 2017), reaching only one meter of total length. Due to our poor understanding of ontogenetic changes, some authors have questioned the degree of maturity of these small-sized 'dwarf' aetosaurs, as some taxa could represent an early ontogenetic stage of another larger species (Heckert & Lucas 2002a, Martz 2002, Schoch 2007, Parker et al. 2008, Roberto-da-Silva et al. 2014,

Parker 2016a, Schoch & Desojo 2016, Heckert et al. 2017, Hoffman et al. 2019, Marsh et al. 2020).

The mid-sized early diverging aetosaur *Aetosauroides* is represented by several individuals collected in two Late Triassic units of South America: the Ischigualasto Formation, Ischigualasto-Villa-Unión Basin, in Argentina (Casamiquela 1960, 1961, 1967, Martinez et al. 2012, Desojo et al. 2020), and the Candelária Sequence, Santa Maria Supersequence (*sensu* Horn et al. 2014), in Southern Brazil (Lucas & Heckert 2001, Da-Rosa & Leal 2002, Langer et al. 2007, Desojo & Ezcurra 2011, Desojo et al. 2012, Roberto-da-Silva et al. 2014, Brust et al. 2018). Recent improvements on histological data and osteoderm variation studies indicated that *Aetosauroides* achieved sexual maturity very early (e.g. Cerda & Desojo 2011, Taborda et al. 2013, Cerda et al. 2018), when they reached about one meter of total length, although putative males are known to attain more than two meters in length (Taborda et al. 2015). Nevertheless, details of its axial morphology and its axial intraspecific variation remain poorly understood (Casamiquela 1960, 1961, 1967, Heckert & Lucas 2002b, Desojo 2005, Desojo & Ezcurra 2011).

Vertebral characters were considered relevant taxonomically as they separate *Aetosauroides* from *Stagonolepis* (Casamiquela 1961, Desojo 2005, Desojo & Ezcurra 2011, Desojo et al. 2012, Parker 2016a), previously suggested as synonyms (e.g. Lucas & Heckert 2001, Heckert & Lucas 2002b). Among these features is a well-rimmed lateral fossa (Fig. 1), the centra of the

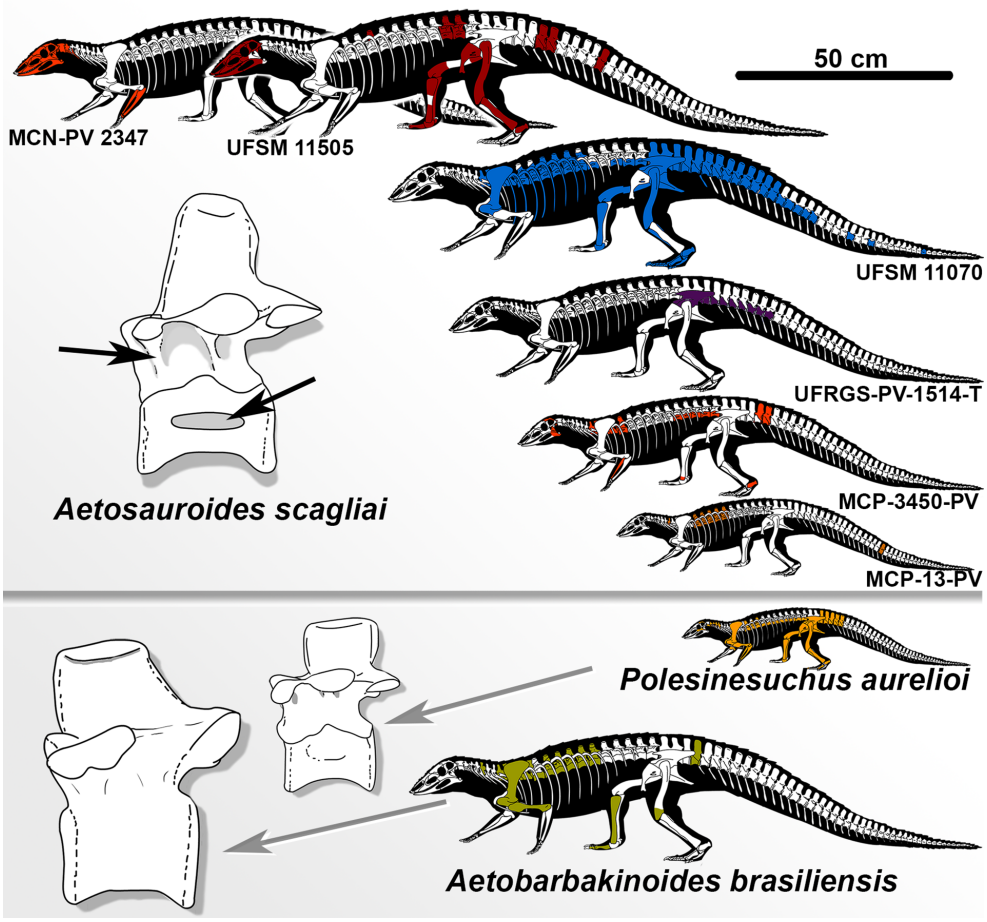

Figure 1. Reconstruction of the Brazilian aetosaurs *Aetosauroides*, *Aetobarbakinoides* and *Polesinesuchus* (without osteoderms and gastralia), and respective schematic drawing of a trunk vertebra in lateral view (not to scale). Colored bone elements are those available on each specimen. Black arrows indicate important characters found in *Aetosauroides*, the infradiapophyseal laminae at the neural arch and the marked lateral fossa at the centra. Specimen size obtained relative to their femur circumference (see Taborda et al. 2013) and trunk vertebrae length (this study).

presacral vertebrae, is considered diagnostic of *Aetosauroides* (Desojo & Ezcurra 2011). The lack of this feature was used to recognize two other small-sized supposedly endemic species in Brazil (Fig. 1), which are only represented, so far, by their type materials: *Aetobarbakinoides brasiliensis*, based on a poorly preserved non-juvenile specimen (Desojo et al. 2012, Cerda et al. 2018); and *Polesinesuchus aurelioi*, based on an immature individual (Roberto-da-Silva et al. 2014). However, intraspecific variation is almost unknown in the axial skeleton of *Aetosauroides*.

In the present contribution we describe in detail the axial skeleton of five specimens of *Aetosauroides* collected in Brazil, allowing a detailed comparative study with other aetosaurs including both endemic *Polesinesuchus* and *Aetobarbakinoides* to discuss their taxonomic validity. Also, for the first time, we perform a histological description of the paramedian osteoderm of *Polesinesuchus* with the aim of accessing the ontogenetic stage of its holotype. Our findings are discussed in an integrated approach relative to the current understanding of the ontogeny and phylogeny of aetosaurs in order to shed light on the taxonomy of the group.

Institutional Abbreviations

CAPPA/UFSM, Centro de Apoio à Pesquisa Paleontológica da Quarta Colônia, Universidade Federal de Santa Maria, São João do Polêsine, Brazil; **CPEZ**, Coleção Municipal, São Pedro do Sul, Rio Grande do Sul, Brazil; **MCN**, Coleção de Paleontologia de Vertebrados, Secretaria Estadual do Meio Ambiente, Porto Alegre, Rio Grande do Sul, Brazil; **MCP**, Museu de Ciências e Tecnologia da Pontifícia Universidade Católica do Rio Grande do Sul, Porto Alegre, Rio Grande do Sul, Brazil; **MCZ**, Museum of Comparative Zoology, Harvard University, Cambridge, Massachusetts, USA; **NCSM**, North Carolina State Museum, Raleigh, North Carolina, USA; **NMS**, National Museum of Scotland, Edinburgh, Scotland; **MNA**, Museum of Northern Arizona, Flagstaff, Arizona, USA; **PEFO**, Petrified Forest National Park, Petrified Forest, Arizona, USA; **PULR**, Paleontología Museo de Ciencias Naturales, Universidad Nacional de La Rioja, La Rioja, Argentina; **PVL**, Paleontología de Vertebrados, Instituto 'Miguel Lillo', San Miguel de Tucumán, Tucumán, Argentina; **SMNS**, Staatliches Museum für Naturkunde, Stuttgart, Germany; **TMM**, Texas Memorial Museum, Austin, Texas, USA; **TTU-P**, Museum of Texas Tech, Lubbock, Texas, USA; **UCMP**, University of California, Berkeley, California, USA; **UFRGS-PV**, Coleção do Laboratório de Paleontologia de Vertebrados, Universidade Federal do Rio Grande do Sul, Porto Alegre, Rio Grande do Sul, Brazil; **UFSM**, Laboratório de Estratigrafia e Paleobiologia of Universidade Federal de Santa Maria, Santa Maria, Rio Grande do Sul, Brazil; **ULBRAPV**, Universidade Luterana do Brasil, Coleção de Paleovertebrados, Canoas, Rio Grande do Sul, Brazil; **UMMP**, University of Michigan, Ann Arbor, Michigan, USA; **UNC**, Department of Geological Sciences, University of North Carolina at Chapel Hill (alocated at NCSM); **USNM**, National Museum of Natural History, Smithsonian Institution, Washington, D.C., USA; **ZPAL AbIII**, Institute of Paleobiology of the Polish Academy of Sciences, Warsaw, Poland.

GEOLOGICAL AND PALEONTOLOGICAL SETTINGS

Brazilian aetosaur materials (Fig. 1) were recovered from the mudstones and fine-grained sandstones layers of the lower portion of the Candelária Sequence, a third-order sequence of the Santa Maria Supersequence (*sensu* Horn et al. 2014), that crops out at the center of the Rio Grande do Sul State. All aetosaur bearing-sites

are associated with the *Hyperodapedon* Assemblage Zone (AZ), which yields the richest tetrapod diversity of the Brazilian Triassic (Schultz et al. 2020). This AZ is correlated with the *Herrerasaurus-Exaeretodon-Hyperodapedon* AZ from the lower levels of the Ischigualasto Formation (Cancha de Bochas Member) from the San Juan Province, Argentina (Langer et al. 2007, Martinez et al. 2012). Recent reassessments of the age estimations indicate an age of approximately 230-221 Ma for the Ischigualasto levels (Desojo et al. 2020) and a mean age of 233 Ma for the Cerro do Alemoa Site, also referred to the *Hyperodapedon* AZ (Langer et al. 2018), which thus represent late Carnian layers.

The analyzed specimens were collected at the Piche Site (Fig. 2d) and the Faixa Nova Area (Fig. 2a-c), distant in nearly 30 km. The specimen MCN-PV 2347 represents the *Aetosauroides* specimen referred in Langer et

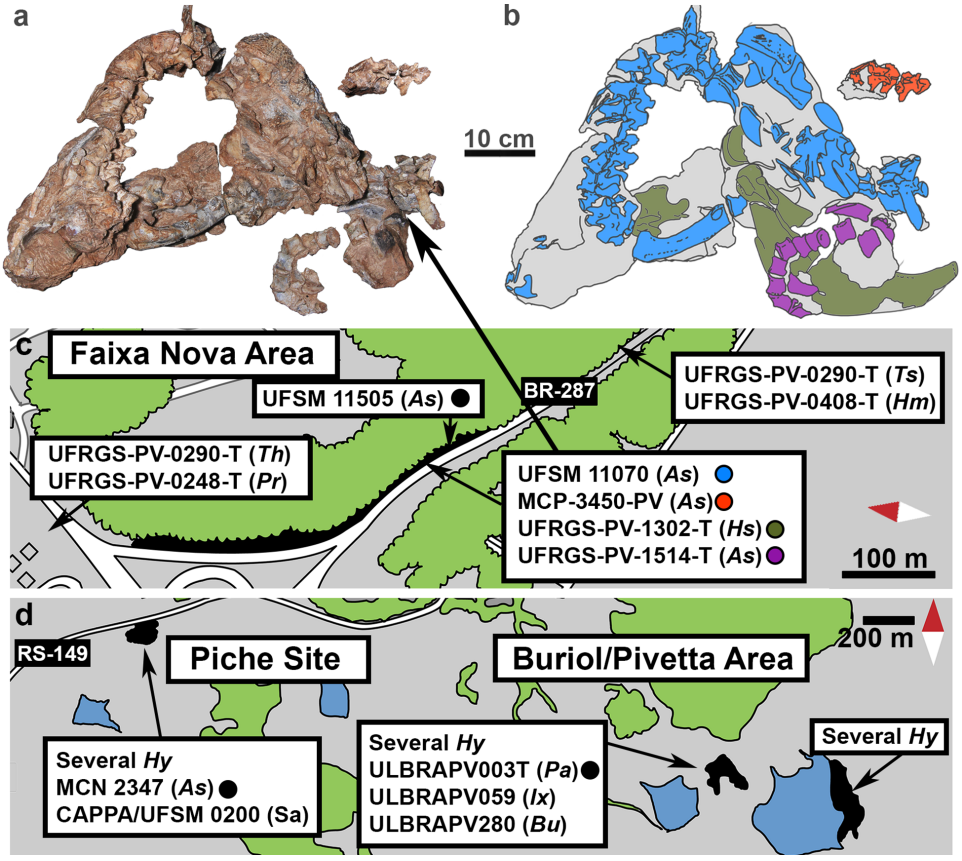

Figure 2. Associated aetosaur individuals and maps of Candelária Sequence outcrops. a, association of three aetosaur *Aetosauroides* (MCP-3450-PV, UFRGS-PV-1514-T and UFSM 11070) and at least one *Hyperodapedon sanjuanensis* (UFRGS -PV-1302-T). b, interpretative drawing. c, Faixa Nova Area with highlighted collected specimens. d, São João do Polêsine Area, with highlighted collected specimens in Piche and Buriol outcrops. Dots reveal studied specimens. Dark areas in the maps indicate the outcrops, green areas fragments of vegetation and blue lakes. Abbreviations: *As*, *Aetosauroides* (aetosaur); *Bu*, *Buriolestes* (dinosaur); *Hy*, *Hyperodapedon* sp. (rhynchosaur); *Hs*, *Hyperodapedon sanjuanensis* (rhynchosaur); *Hm*, *Hyperodapedon mariensis* (rhynchosaur); *Ix*, *Ixalerpeton* (lagerpetid); *Pa*, *Polesinesuchus* (aetosaur); *Pr*, *Prozostrodon* (cynodont); Sa, sauropodomorph indet. (dinosaur); *Th*, *Therioherpeton* (cynodont); *Ts*, *Teyumbaita* (rhynchosaur).

al. (2007) from mudstone layers of the Piche Site (Fig. 2d). This outcrop has yielded a record of conchostrachans, sauropodomorph dinosaurs, hyperodapedontinae rhynchosaurs and fish remains (see Garcia et al. 2019).

The Faixa Nova Area represents a series of road-cut outcrops, also known as Cerrito I, II and III (see Da-Rosa 2004, 2015), within Santa Maria city (Camobi neighborhood), Rio Grande do Sul State, Brazil (Da-Rosa & Leal 2002, Brust et al. 2018). The Faixa Nova (Cerrito I) specimens (UFRGS-PV-1514-T, UFSM 11070, UFSM 11505 and MCP-3450-PV) were recovered at the lower massive mudstone levels, where the rhynchosaur *Hyperodapedon mariensis* (UFRGS-PV-0408-T) was also found (Da-Rosa & Leal 2002, Da-Rosa 2004, Desojo & Ezcurra 2011). Remarkably, all these aetosaurs specimens were found within a 10 m² area, three of which (UFRGS-PV-1514-T, UFSM 11070 and MCP-3450-PV) were associated with *H. sanjuanensis* (UFRGS-PV-1302-T) (Fig. 2a-b), with elements mixed over each other. The specimen UFSM 11505 was found no more than 10 meters away, but the lack of precise stratigraphic context precludes us from establishing with confidence if it was found at the same layer. This represents the first aetosaur association reported for South America.

Da-Rosa & Leal (2002) preliminarily reported the specimen UFSM 11070, which was referred to *Aetosauroides scagliai* by Desojo and Ezcurra (2011), being housed by two other institutions (Desojo & Ezcurra 2011) with distinct numbers: MCP-3450-PV and UFRGS-PV-1302-T (Fig. 2b). However, detailed preparation of the UFRGS-PV-1302-T sample revealed that at least three aetosaur individuals are present (Fig. 2b), plus three rhynchosaur individuals (see item 2 of Supplementary Material - Fig. S2). Most elements housed at MCP represent a distinct smaller *Aetosauroides* individual, not related to the other two housed at UFRGS. We therefore restrict the number MCP-3450-PV to the smaller specimen, and UFSM 11070 to the larger and most complete individual. A new number, UFRGS-PV-1514-T, was created for the third and intermediate in size specimen, and the number UFRGS-PV-1302-T is now restricted to the rhynchosaur material.

MATERIALS AND METHODS

Specimens examined

We describe in detail the axial skeleton of five *Aetosauroides* individuals (MCN-PV 2347, MCP-3450-PV, UFSM 11070, UFSM 11505 and UFRGS-PV-1514-T), using computed tomographic (CT) scan images for a more comprehensive morphological description of axial elements. See item 4 of the Supplementary Material for full description, including for the morphology of the ribs and hemal arches (Fig. S5). We also review the axial osteology of *Polesinesuchus* (ULBRAPV003T) and *Aetobarbakinoides* (CPEZ 168) and compare those specimens with other aetosaur and key non-aetosaur archosaur materials (Supplementary Material – Table SI).

The specimens MCP-3450-PV, UFSM 11070 and UFSM 11505 were previously recognized as *Aetosauroides* (e.g. Desojo & Ezcurra 2011, Brust et al. 2018), whereas MCN-PV-2347 is here referred for the first time based on its cervical vertebrae and skull features. We have identified, as a possible new autapomorphy for *Aetosauroides*, the marked lateral fossae on the centra of the anterior caudal vertebrae, as this feature is present in the type material of *Aetosauroides* (PVL 2073) and in the largest specimen PVL 2052. This allows the specimen UFRGS-PV-1514-T, mostly represented by its caudal series, to also be referred to *Aetosauroides*. As the total length of most *Aetosauroides* individuals are around 1.3 meters (PVL 2059, PVL 2073, MCN-PV 2347, UFSM 11070 and UFSM 11505; see also Taborda et al. 2013) we will refer as small-sized individuals

those with less than 1.3 meter of total length (e.g. MCP-13-PV, MCP-3450-PV and UFRGS-PV-1514-T), and as large-sized those over 2 meters (e.g. PVL 2052 and PVL 2091).

Procedures

Pneumatic hammers and needles were used in the preparation of the specimens, as well as acetic acid diluted in water and consolidant (ethyl methacrylate copolymer B-72). Several measurements were obtained (see item 1 of the Supplementary Material, Fig. S1 and Tables SI-SVII) using an analog caliper. A Bruker SkyScan 1173 microtomographer (Laboratório de Sedimentologia e Petrologia, Instituto de Petróleo e dos Recursos Naturais, Pontifícia Universidade Católica do Rio Grande do Sul), using a source voltage of 130 kV and a current of 61 uA, was used to scan the specimen MCN-2347, as the cervical series is mostly covered by other bones and matrix. This allowed us to digitally isolate the axial elements using the software 3d Slicer v4 (Fedorov et al. 2012).

In order to estimate the age of the type material of *Polesinesuchus* we made a thin-section of a paramedian osteoderm to compare with other previously sampled *Aetosauroides* and *Aetobarbakinoides* specimens (Cerda & Desojo 2011, Taborda et al. 2013, Scheyer et al. 2014, Cerda et al. 2018). We followed the methods proposed by Cerda & Desojo (2011), Taborda et al. (2013) and Chinsamy & Raath (1992). The preparation of the histological section was carried out in the Laboratório de Paleontologia de Vertebrados, Centro de Estudos em Petrologia e Geoquímica and in the Centro de Microscopia e Microanálise of Universidade Federal do Rio Grande do Sul (Brazil). The paramedian osteoderm was photographed and standard measurements were taken prior sectioning (e.g. length and width). It was embedded in a low viscosity polyester resin (Redelease© SKU: ECF12863) and then sectioned near the target region a longitudinal section near the dorsal eminence. This region was then mounted on glass, which was grounded and polished. The thin-section was analyzed using a Zeiss© Axio Scope.A1 (at UFRGS-PV), and the photographs were combined using Adobe Photoshop© vCS6. The terminology of the histologic description followed Francillon-Vieillot et al. (1990), Cerda & Desojo (2011) and Cerda et al. (2018). The high-resolution whole-slide histological images and the CT-Scan images were uploaded on the Morphobank online repository (O'Leary & Kaufman 2012) at the access link http://morphobank.org/permalink/?P3778.

RESULTS

Comparative description

Atlas (Fig. 3)

The atlas is preserved in the *Aetosauroides* specimens MCN-PV 2347 and the small-sized MCP-3450-PV, being here described for the first time. The atlantal intercentrum is small (Fig. 3a1-2) and quadrangular in lateral view (Fig. 3a1), presenting a shallow fossa in its lateral surface (Fig. 3a1: lfo). It represents less than half of the length of the axial centrum (see Table S03), with a slight concave anterior and posterior margins (Fig. 3a1-2). Two short lateral projections for the articulation of the first cervical rib are present posteriorly (Fig. 3a1: ra). Ventrally, no keel is present, but the surface is rugose with small pits and foramens (Supplementary Fig. S4e). The Y-shaped neural arch of the atlas is preserved in MCN-PV 2347 (Fig. 3a1: na), presenting an acute epipophysis, a feature common in other pseudosuchians (e.g. *Prestosuchus chiniquensis*, UFRGS-PV-0629-T; *Effigia*, AMNH 30587, Nesbitt 2007), but difficult to identify in aetosaurs, as

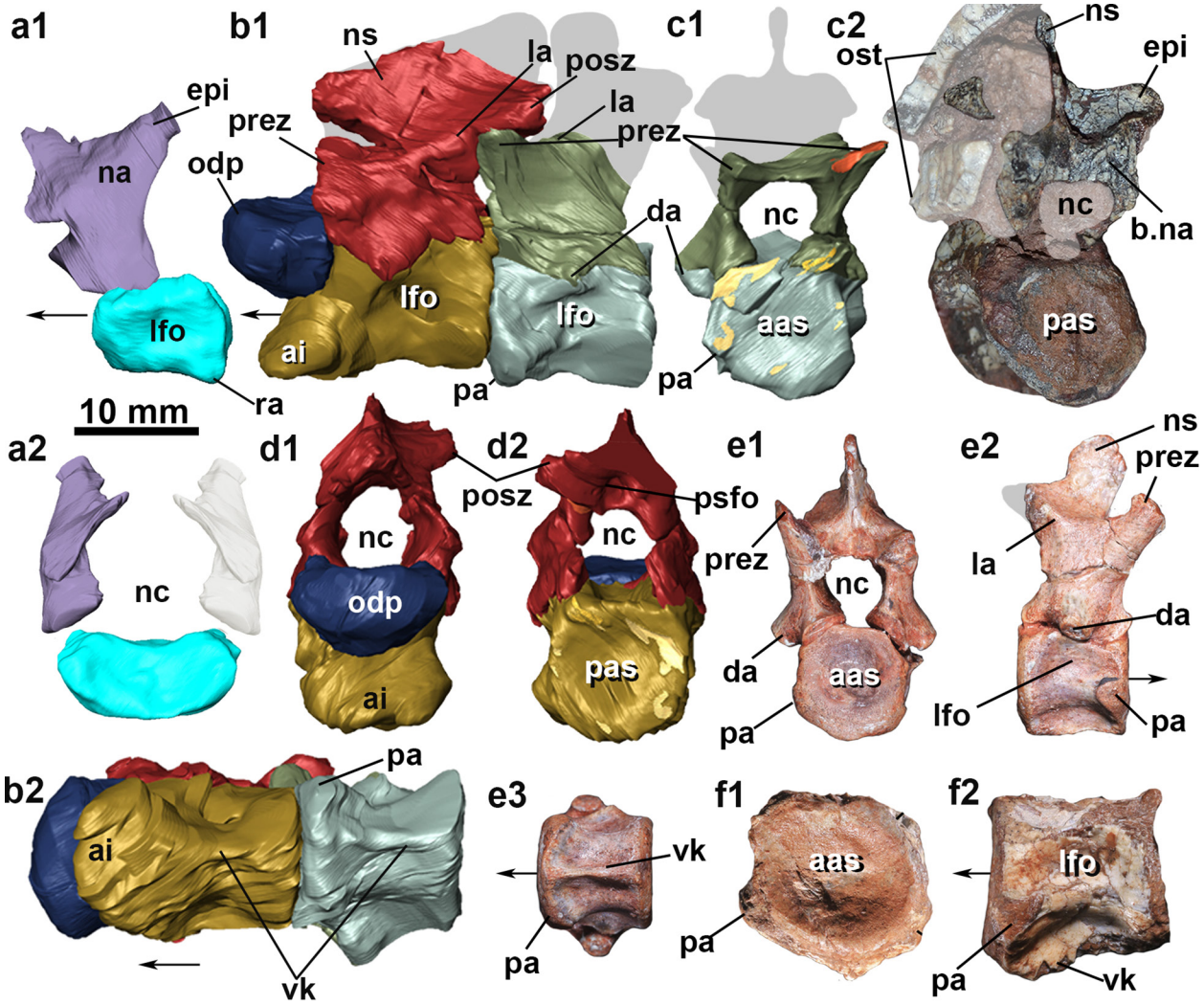

Figure 3. Cervical vertebrae of *Aetosauroides* (MCN-PV 2347 and UFSM 11070) and *Polesinesuchus* (ULBRAPV003T). a, left atlas neural arch and atlas intercentrum of MCN-PV 2347 in lateral (a1) and anterior views (a2). b, axis and third vertebra in lateral (b1) and ventral view (b2). c, third vertebra of MCN-PV 2347 in anterior (c1) and posterior views (c2). d, axis of MCN-PV 2347 in anterior (d1) and posterior views (d2). e, complete fourth (?) cervical vertebrae of *Polesinesuchus* type material in anterior (e1), lateral (e2) and ventral views (e3). f, cervical centra of *Aetosauroides* UFSM 11070 in anterior (f1) and in left lateral views (f2). Arrow indicates anterior direction. Abbreviations: aas, anterior articular surface; ai, axis intercentrum; b., broken; da, diapophysis; epi, epipophysis; la, lamina; lfo, lateral fossa; na, neural arch; nc, neural canal; ns, neural spine; odp, odontoid process; ost, osteoderm; pa, parapophysis; pas, posterior articular surface; prez, prezygapophyses; psfo, postspinal fossa; posz, postzygapophyses; ra, articular facet for the atlas rib; vk, ventral keel.

they are generally broken (e.g. *Typothorax*; TTU-P 9214) or hidden by matrix (*Sierritasuchus*, UMMP V60817; *Desmatosuchus spurensis,* UMMP V7476).

Axis (Fig. 3)

The axis is preserved in MCN-PV 2347, being elongated anteroposteriorly, like most aetosaurs. It bears a ventral keel, unlike Desmatosuchini aetosaurs (e.g. *Longosuchus*, TMM 3485-97; *D. smalli*, TTU-P 9205; *D. spurensis*, UMMP V7476; Case 1922; *Sierritasuchus*, UMMP V60817; Parker et al. 2008). A pronounced odontoid process (atlantal pleurocentrum; Fig. 3b1: odp) and axis intercentrum (Fig. 3b2: ai) are present, both

measuring one-third of the length of the axis. In *Polesinesuchus* the odontoid process is poorly preserved (as indicated by Roberto-da-Silva et al. 2014) and the axis intercentrum is missing. The 'U-shaped articulation facet' described by Roberto-da-Silva et al. (2014) represents in fact the articulation area with the atlas intercentrum, which is disarticulated in *Polesinesuchus*. The neural arch of MCN-PV 2347 is not fused to the centrum and has an anteroposteriorly elongated (four times the third cervical neural spine length) and posteriorly tall neural spine (Fig. 3b1: ns). The prezygapophyses are reduced and hemicircular in lateral view (Fig. 3b1: prez). They are placed dorsally to the odontoid process but do not extend beyond the anterior border of the axis centrum (Fig. 3b1). An interzygapophyseal lamina connects the prezygapophyses to the postzygapophyses of the axis (Fig. 3b1: la). The postzygapophyses are posteriorly elongated, extending over the third cervical vertebra posterior border (Fig. 3b1: posz). A post-spinal fossa is present in the axis (Fig. 3d2: psfo).

Postaxial cervical series (Fig. 3)

In MCN-PV 2347 the third cervical vertebra is well preserved, and the fourth is represented by its neural arch cut in half (Fig. 3c2: b.na). Five fragmentary cervical centra were found associated with UFSM 11070 (Fig. 3f1-2). In all of the available cervical vertebrae of MCN-PV 2347 and UFSM 11070 the neural arches are not fused to the centra (Fig. 3b1 and 3f), and all present a developed ventral keel (Fig. 3b2 and 3f2: vk), and a lateral fossa at the lateral surface of the centrum (Fig. 3b1 and 3f2: lfo), ventral to the neurocentral suture, both features described for the Argentine *Aetosauroides* specimens (e.g. Desojo 2005, Desojo & Ezcurra 2011, Desojo et al. 2012, Ezcurra 2016). Unlike what was stated by Roberto-da-Silva et al. (2014), a homologous lateral fossae is present in the cervicals of *Polesinesuchus* (Fig. 3e2: lfo), although less developed when compared with *Aetosauroides* (UFSM 11070 and MCP-PV 2347). As indicated by Roberto-da-Silva et al. (2014) the ventral keel is present in *Polesinesuchus* (Fig. 3e3: vk), being absent in *Aetobarbakinoides* (Desojo et al. 2012). Additionally, unlike *Typothorax* (Martz 2002), the parapophysis of the *Aetosauroides* UFSM 11070 (Fig. 3f: pa) and in MCN-PV 2347 (Fig. 3b1 and 3c1: pa) are not placed on a stalk, instead are just slightly laterally projected. The parapophysis is anteriorly projected and the postzygapophysis posterolaterally projected, with a short epipophysis (Fig. 3c2: epi). An isolated centra of MCP-3450-PV (Fig. 4i-j) may represent the last cervical as the parapophysis is placed near the neurocentral suture, but it presents a flat ventral surface with two longitudinal faint keels (Fig. 4j: vk), structures not common among aetosaurs (such as *Neoaetosauroides*, PVL 3525).

Trunk vertebrae

Previous authors have described *Aetosauroides* trunk vertebrae as being amphicoelous, spool-shaped and anteroposteriorly long (Casamiquela 1961, Desojo & Ezcurra 2011), all conditions present in the specimens UFSM 11070, UFSM 11505 and the small-sized MCP-3450-PV. In UFSM 11070 (Fig. 4a and 4b) a series of ten articulated trunk vertebrae are preserved, with at least five disarticulated subsequent vertebrae. Most anterior centra of UFSM 11070 are covered by matrix and other elements (e.g. osteoderms and ribs) precluding us from determining their full morphology. In MCP-3450-PV at least thirteen trunk centra are present (mostly isolated), including three with associated neural arches and four fragmentary isolated neural arches (Fig. 2a-b). Only two posterior trunk vertebrae are available for UFSM 11505, representing

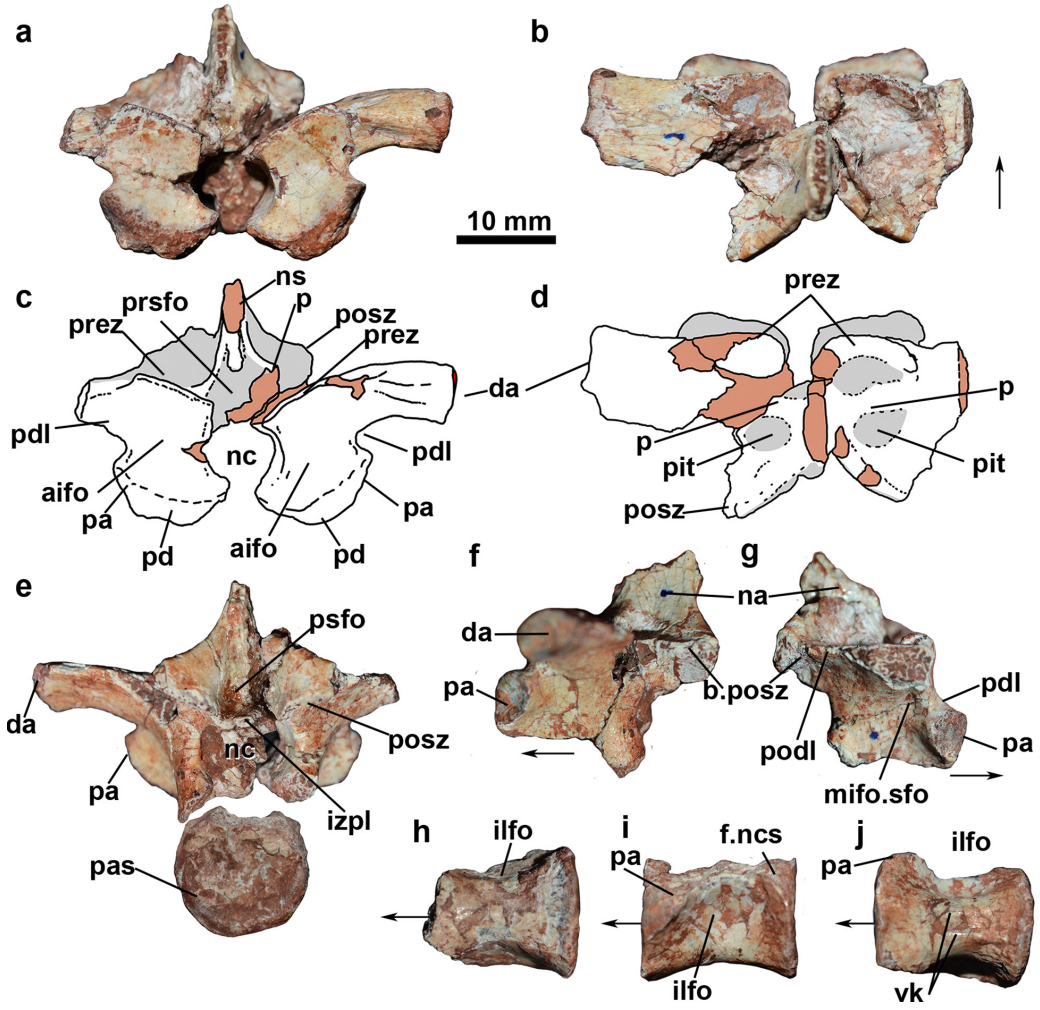

Figure 4. Last cervical and anterior trunk vertebrae of *Aetosauroides* (MCP-3450-PV). Probable transitional vertebrae isolated neural arch in anterior (a), dorsal (b), posterior (e), left lateral (f) and right lateral views (g); with interpretative drawings of the anterior (c) and dorsal (d) views. Compatible isolated centra, in posterior (e) and ventral view (h). Putative last cervical vertebra in lateral (i) and ventral views (j). Arrow indicates anterior direction. Abbreviations: aifo, anterior infradiapophyseal fossae; b., broken; da, diapophysis; f.ncs, facet of the neurocentral suture; ilfo, incipient lateral fossae of the centrum; izpl, intrapostzygapophyseal lamina; mifo.sfo, middle infradiapophyseal fossa with sub-fossa; na, neural arch; nc, neural canal; ns, neural spine; p, pillar-like ridge; pa, parapophysis; pas, posterior articular surface; pd, neural arch peduncle; pdl, paradiapophyseal lamina; pit, deep pit lateral to the neural spine; prez, prezygapophyses; prsfo, prespinal fossa; psfo, postspinal fossa; podl, posterior zygodiapophyseal lamina; posz, postzygapophyses; vk, ventral keel.

probably the last trunk vertebrae. All available trunk vertebrae of these specimens present open neurocentral sutures.

The trunk vertebrae of UFSM 11070, UFSM 11505 and the small-sized MCP-3450-PV are moderately tall, but longer than the cervicals, with the height of the neural arch of two to three times that of the centra (see Table S5), similar to what was observed by Desojo & Ezcurra (2011) for PVL 2073 and the small-sized MCP-13-PV. The oval parapophysis is placed in the neural arch close to the neurocentral suture in the anteriormost trunk vertebrae of MCP-3450-PV (Fig. 4a-g: pa) and UFSM 11070 (Fig. 5e

and 5f: pa), being connected to the ellipsoid diapophysis by a paradiapophyseal lamina (Fig. 4c and 4g: pdl). This lamina delimits anteriorly a middle infradiapophyseal fossa, which also bears a shallow subfossa at least in the MCP-3450-PV trunk vertebrae (Fig. 4g: mifo.sfo). These anteriormost available neural arches seem to represent the transitional vertebrae between the cervical and the trunk of both specimens, as the parapophysis is just dorsal to the neurocentral suture (see Parker 2018b).

The parapophysis of the fourth available trunk vertebra in UFSM 11070 is almost in the same horizontal plane as the diapophysis, but well displaced ventromedially (Fig. 5b-c: pa). The parapophysis and the diapophysis remain separated by a groove in more posterior vertebrae (Fig. 6c: gap), as observed by Casamiquela (1961) in the type specimen PVL 2073. In contrast, the parapophysis is located at a higher level in relation to the diapophysis in some aetosaurs (for instance *Scutarx*, PEFO 34045; *Paratypothorax* sp., TTU-P 9416). Also, in the anteriormost trunk vertebrae of the small-sized MCP-3450-PV (Fig. 4a) and UFSM 11070 the transverse process is laterally oriented (TV1, Fig. 5e-f: tp). However, it becomes progressively more dorsolaterally oriented in subsequent vertebrae (TV6, Fig. 7a2), but returning a more laterally oriented condition at the posteriormost trunk (TV7, Fig. 7b2) in UFSM 11070 (unknown in MCP-3450-PV). This resembles the condition of

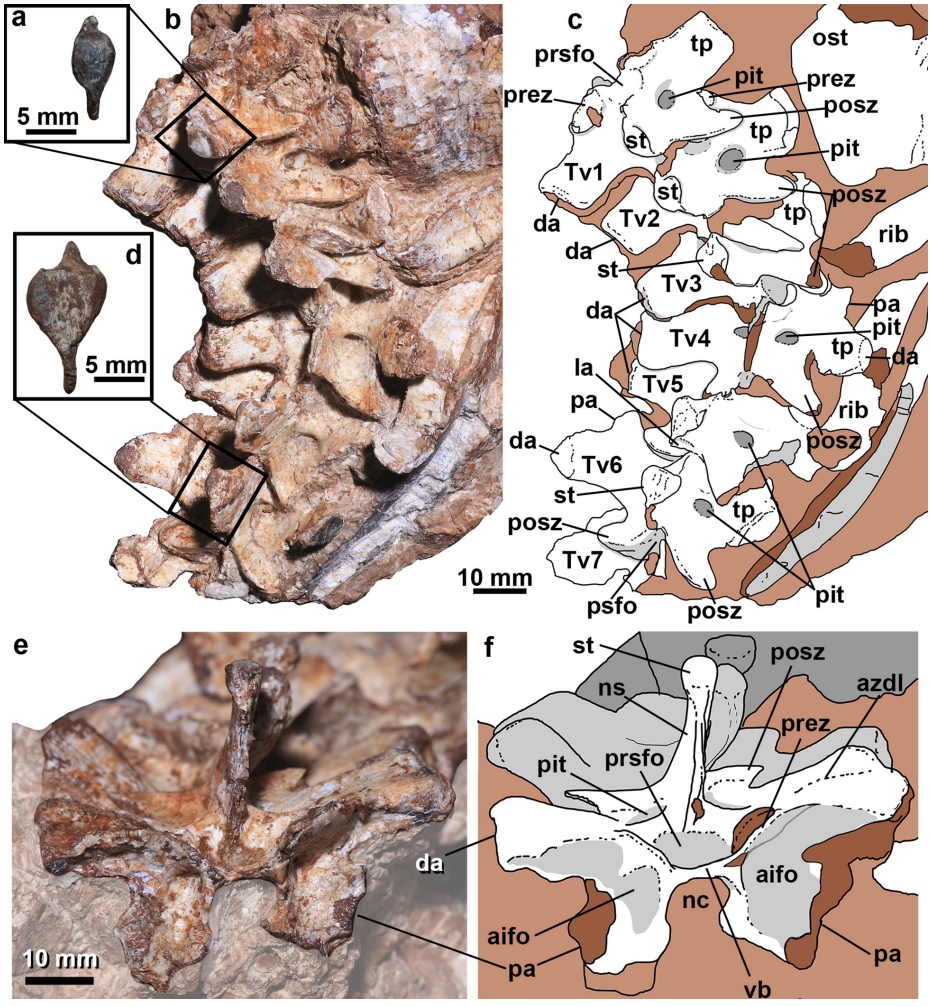

Figure 5. Anterior trunk vertebrae of *Aetosauroides* (UFSM 11070). a, detail of the drop-shaped spine table, in dorsal view. b, anterior trunk articulated series in dorsal view, and its interpretative drawing (c). d, detail of the heart-shaped spine table, in dorsal view. e, anteriormost preserved trunk neural arch in anterior view and interpretative drawing (f). Abbreviations: aifo, anterior infradiapophyseal fossae; azdl, anterior zygodiapophyseal lamina; da, diapophysis; la, lamina; nc, neural canal; ns, neural spine; ost, paramedian osteoderm fragment; pa, parapophysis; pit, deep pit lateral to the neural spine; prez, prezygapophyses; prsfo, prespinal fossa; psfo, postspinal fossa; posz, postzygapophyses; psfo, post-spinal fossa; st, spine-table; tp, transverse process; Tv, trunk vertebra; vb, ventral bar.

most other aetosaurs described previously (e.g. Casamiquela 1961, Walker 1961), but seem to not occur in *Scutarx* (PEFO 34045), *Typothorax* (Martz 2002) and *Desmatosuchus spurensis* (MNA V9300 and UMMP V7476) were the transversal process seem to remain laterally oriented through the series.

The prezygapophyses in the trunk vertebrae are latero-medially expanded and located at the base of the transverse process in the small-sized MCP-3450-PV and UFSM 11070, being slightly elevated by a shallow platform in most vertebrae (Fig. 4-9: prez) and steeply inclined medially, as in other *Aetosauroides* (Desojo & Ezcurra 2011). The postzygapophyses are longer than the prezygapophyses in MCP-3450-PV and UFSM 11070, extending until the mid-length of the subsequent vertebra, and are well divergent laterally (Fig. 4-9: posz). Desojo & Ezcurra (2011) indicate that this condition is an autapomorphy of *Aetosauroides* (PVL 2052, PVL 2073 and MCP-13-PV), where the ratio of the length and width between the tips are lower than 0.75. This is the condition present in UFSM 11070 (0.24 to 0.56) and the small-sized MCP-3450-PV (0.36 to 0.50) and, interestingly, also in *Polesinesuchus* (0.38;

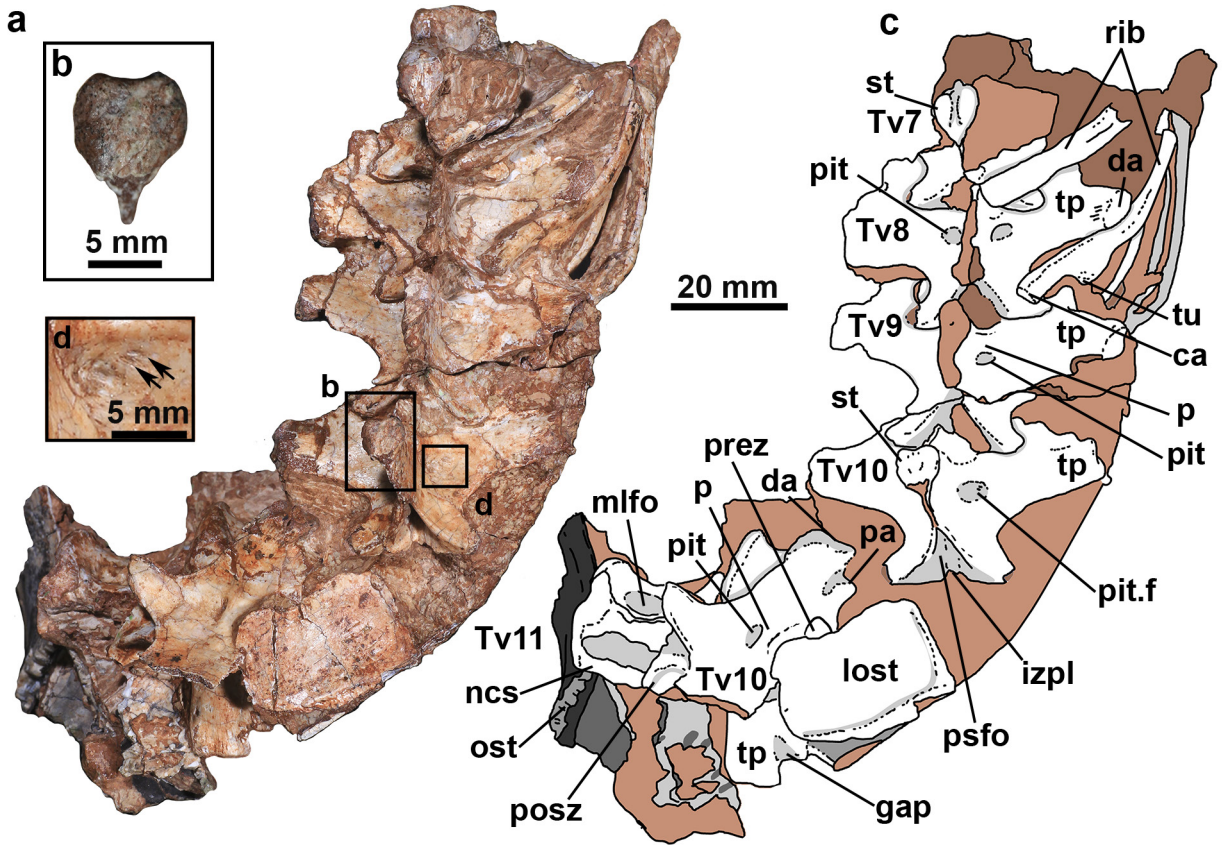

Figure 6. Mid- and posterior trunk vertebrae of *Aetosauroides* (UFSM 11070). a, articulated series of mid- to posterior trunk vertebrae in dorsal view and interpretative drawing (c). b, detail of the heart-shaped spine table, in dorsal view. d, detail of the lateral pit with foramina present. Abbreviations: ca, capitulum; da, diapophysis; gap, groove separating the parapophysis from the diapophysis; izpl, intrapostzygapophyseal lamina; lost, lateral osteoderm; mlfo, wel-rimmed lateral fossae of the centrum; ncs, neurocentral suture; ost, paramedian osteoderm fragment; p, pillar-like ridge; pa, parapophysis; pit, deep pocket pit lateral to the neural spine; pit.f, deep pocket pit lateral to the neural spine with foramina; prez, prezygapophyses; psfo, postspinal fossa; posz, postzygapophyses; st, spine-table; tp, transverse process; tu, tuberculum; Tv, trunk vertebra.

not noticed by Roberto-da-Silva et al. 2014). A sharp postzygodiapophyseal lamina connects the postzygapophyses with the diapophysis in all specimens (Fig. 4g, 7b3, 7d, 8e, 9a, 9b4: podl). The postzygodiapophyseal lamina forms the dorsal limit of a posterior infradiapophyseal fossa in the small-sized MCP-3450-PV (Fig. 9a and 9b4: pifo) and in UFSM 11070 (Fig. 7b3 and 7d: pifo), like in *Polesinesuchus* (Fig. 10b: pifo) and *Stagonolepis robertsoni* (Walker 1961).

In the anteriormost trunk vertebrae of the small-sized MCP-3450-PV, both the anterior (acdl) and posterior (pcdl) centrodiapophyseal lamina are absent (Fig. 4g). However, in the

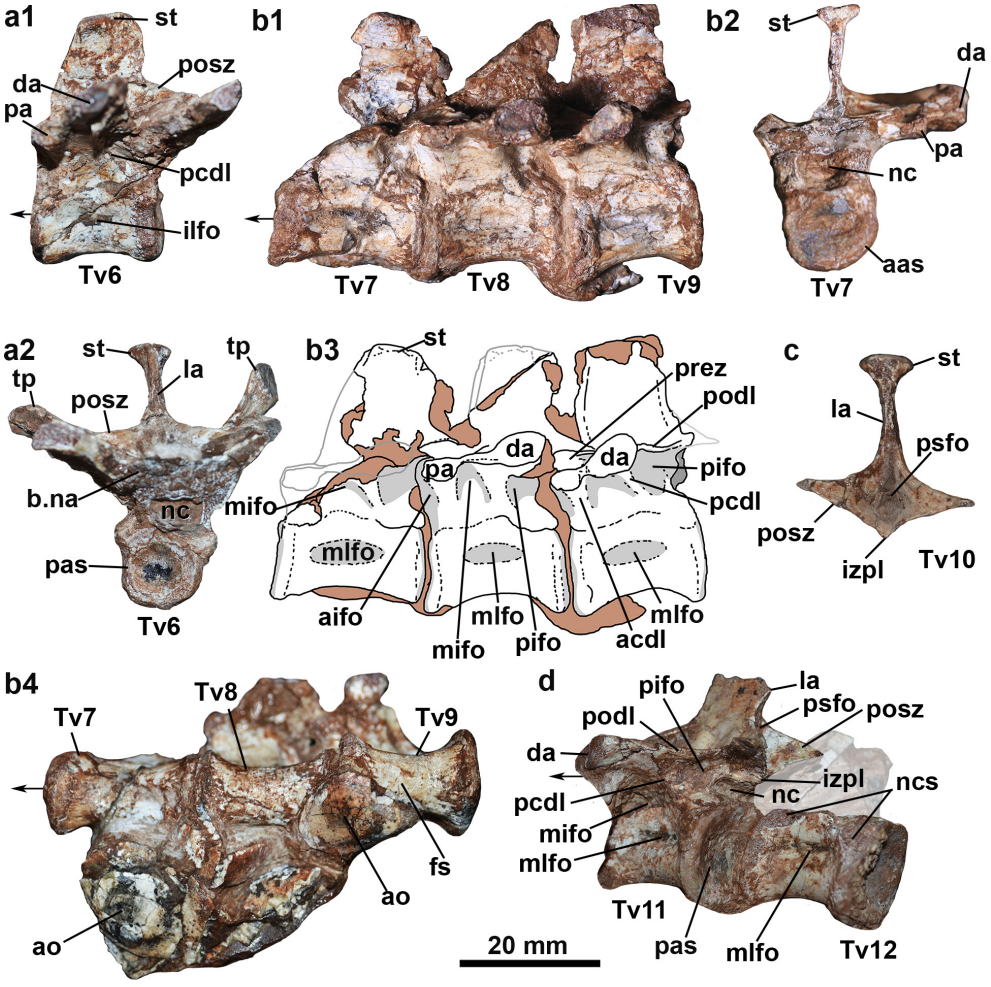

Figure 7. Details of the mid- to posterior trunk vertebrae of *Aetosauroides* (UFSM 11070). a, sixth trunk vertebra (Tv6) in lateral (a1) and posterior (a2) views. b, seventh to ninth posterior trunk vertebrae (Tv7-9) in lateral (b1) and ventral (b4) views, with interpretative drawing in lateral view (b3). c, tenth trunk vertebra (Tv10) detail of the neural spine and postzygapophysis, in posterior view. d, eleventh and twelfth trunk vertebrae (Tv11-12) in posterolateral view (d). Arrow indicates anterior direction. Abbreviations: aas, anterior articular surface; acdl, anterior centrodiapophyseal lamina; aifo, anterior infradiapophyseal fossae; ao, appendicular osteoderm; b., broken da, diapophysis; fs, flat ventral surface; ilfo, incipient lateral fossae of the centrum; izpl, intrapostzygapophyseal lamina; la, lamina; mifo, middle infradiapophyseal fossa; mlfo, wel-rimmed lateral fossae of the centrum; na, neural arch; nc, neural canal; ncs, neurocentral suture; pa, parapophysis; pas, posterior articular surface; pcdl, posterior centrodiapophyseal lamina; pifo, posterior infradiapophyseal fossa; prez, prezygapophyses; prsfo, prespinal fossa; psfo, postspinal fossa; podl, posterior zygodiapophyseal lamina; posz, postzygapophyses; psfo, post-spinal fossa; st, spine-table; tp, transverse process; Tv, trunk vertebra.

mid-trunk vertebrae of MCP-3450-PV (Fig. 9b3: acdl and pcdl) and UFSM 11070 (Tv6, Fig. 7a1: pcdl), the centrodiapophyseal laminae are incipient and pillar-like in form. In more posterior trunk vertebrae of UFSM 11070 (Tv7-10, Fig. 7b3 and 7d: acdl and pcdl) and UFSM 11505 (Fig. 11e: acdl and pcdl) both centrodiapophyseal laminae are more marked and sharp than in all available vertebrae of the smaller *Aetosauroides* specimens MCP-3450-PV (Fig. 8 and 9) and MCP-13-PV (Fig. 10h). The condition of the posterior trunk of UFSM 11070 and UFSM 11505 resemble the type material of PVL 2073 and PVL 2059, but it still contrasts with the even more marked lamina of PVL 2052, one of the larger *Aetosauroides* specimens (Taborda et al. 2015). In the vertebrae with anterior centrodiapophyseal lamina (including the mid-trunk of MCP-3450-PV) it is possible to observe an incipient anterior infradiapophyseal fossa (Fig. 4c, 7b3, 8e and 9b1:

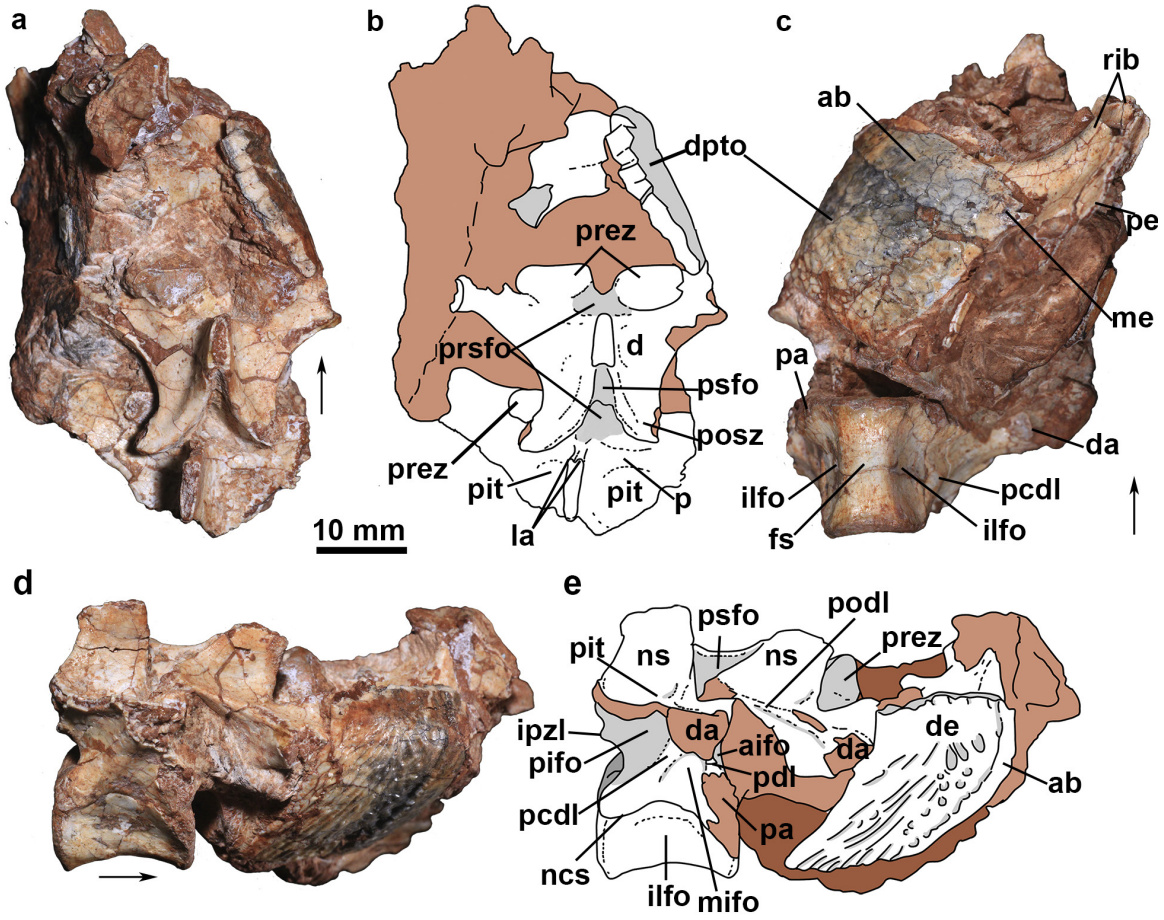

Figure 8. Anterior trunk vertebrae of *Aetosauroides* (MCP-3450-PV). Two articulated vertebrae of MCP-3450-PV in dorsal (a), ventral (c) and right lateral (d). Interpretative drawings of the dorsal (b) and right lateral (e) views. Arrow indicates anterior direction. Abbreviations: ab, anterior bar of the osteoderm; aifo, anterior infradiapophyseal fossae; d, depression; da, diapophysis; de, dorsal eminence of the osteoderm; dpto, dorsal paramedian trunk osteoderm; fs, flat ventral surface; ilfo, incipient lateral fossae of the centrum; izpl, intrapostzygapophyseal lamina; la, lamina; mifo, middle infradiapophyseal fossa; ncs, neurocentral suture; ns, neural spine; p, pillar-like ridge; pa, parapophysis; pcdl, posterior centrodiapophyseal lamina; pdl, paradiapophyseal lamina; pe, posterior expansion of the rib; pifo, posterior infradiapophyseal fossa; pit, deep pit lateral to the neural spine; prez, prezygapophyses; prsfo, prespinal fossa; psfo, postspinal fossa; podl, posterior zygodiapophyseal lamina; posz, postzygapophyses; psfo, post-spinal fossa; Tv, trunk vertebra.

aifo), being shallower than the middle and the posterior infradiapophyseal fossae. A shallow sub-triangular middle infradiapophyseal fossa is concealed between the centrodiapophyseal laminae in MCP-3450 (Fig. 8e: mifo), UFSM 11070 (Fig. 7b3: mifo) and UFSM 11505 (Fig. 11e: mifo), being less marked than the posterior infradiapophyseal fossa.

Although Roberto-da-Silva et al. (2014) have indicated that both centrodiapophyseal laminae were absent in *Polesinesuchus*, first hand inspection by the authors of the type material ULBRAPV003T (Fig. 10b: acdl and pcdl) revealed that it shares the same incipient condition as small specimens of *Aetosauroides*, like the small-sized MCP-3450-PV (Fig. 8e: pcdl) and available trunk vertebrae of compatible in size MCP-13-PV (Fig. 10h: pcdl). In addition, the three infradiapophyseal fossae are markedly present in *Polesinesuchus* (Fig. 10b: mifo and pifo; 10f: aifo). The middle and posterior fossae in some trunk vertebrae of *Polesinesuchus*

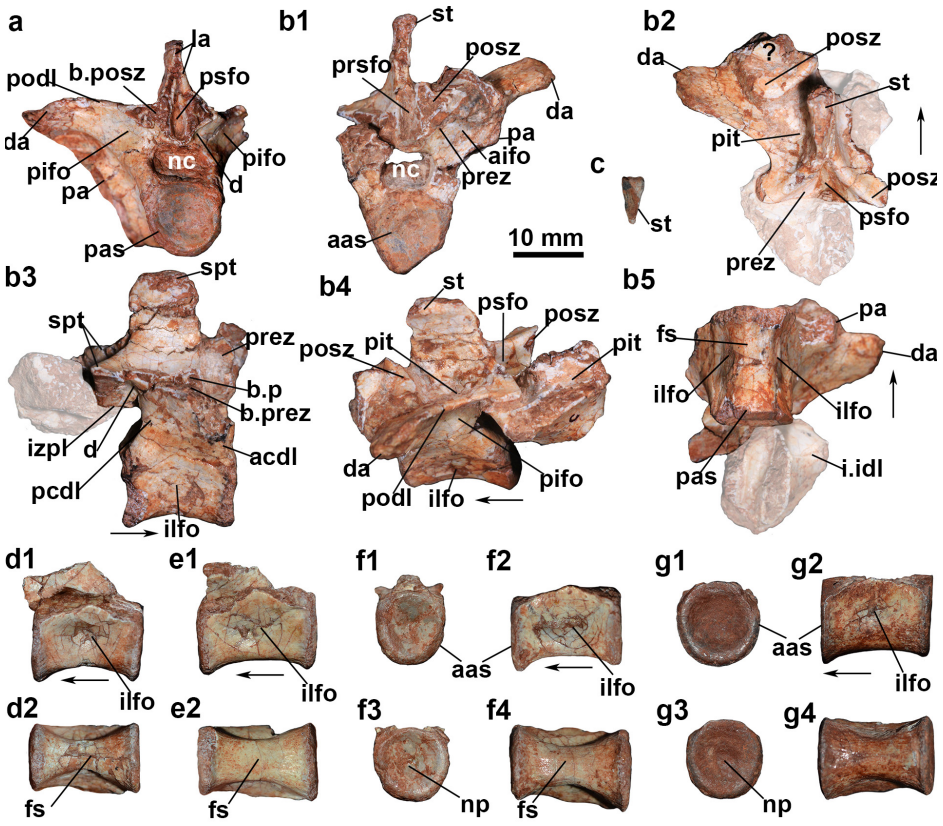

Figure 9. Trunk vertebrae of *Aetosauroides* (MCP-3450-PV). a, the last vertebrae of Figure 9 in posterior view. b, subsequent trunk vertebra in anterior (b1), dorsal (b2), right lateral (b3), dorso-lateral (b4), ventral (b5) views. c, detail of the isolated triangular spine-table, in dorsal view. d, isolated trunk vertebra in lateral (d1) and ventral views (d2). e, isolated trunk vertebra in lateral (e1) and ventral views (e2). f, isolated trunk vertebra in lateral (f1) and ventral views (f2). g, isolated trunk vertebra in lateral (g1) and ventral views (g2). Arrow indicates anterior direction. Abbreviations: aas, anterior articular surface; acdl, anterior centrodiapophyseal lamina; aifo, anterior infradiapophyseal fossae; b, broken; d, depression; da, diapophysis; fs, flat ventral surface; ilfo, incipient lateral fossae of the centrum; izpl, intrapostzygapophyseal lamina; la, lamina; nc, neural canal; np, notochordal pit; odp, odontoid process; ost, paramedian osteoderm fragment; p, pillar-like ridge; pa, parapophysis; pas, posterior articular surface; pcdl, posterior centrodiapophyseal lamina; pifo, posterior infradiapophyseal fossa; pit, deep pit lateral to the neural spine; prez, prezygapophyses; prsfo, prespinal fossa; psfo, postspinal fossa; podl, posterior zygodiapophyseal lamina; posz, postzygapophyses; psfo, post-spinal fossa ; st, spine-table.

are as deep as in UFSM 11070. Conversely, the centrodiapophyseal laminae are absent or incipient in *Aetobarbakinoides* (Desojo et al. 2012), forming a poorly marked fossa.

In MCP-3450-PV (Fig. 4e and 9a: psfo), UFSM 11070 (Fig. 7c: psfo) and UFSM 11505 (Fig. 11c: psfo), a deep postspinal fossa is present. In MCP-3450-PV and UFSM 11070, it is possible to observe that the postspinal fossa is ventromedially concealed by an intrapostzygapophyseal lamina (Fig. 4e and 7c: izpl), which connects both postzygapophyses. The shape of this lamina varies between the specimens, being 'V-shaped' in UFSM 11070 (Fig. 7c-d: izpl), as well as in other Argentine

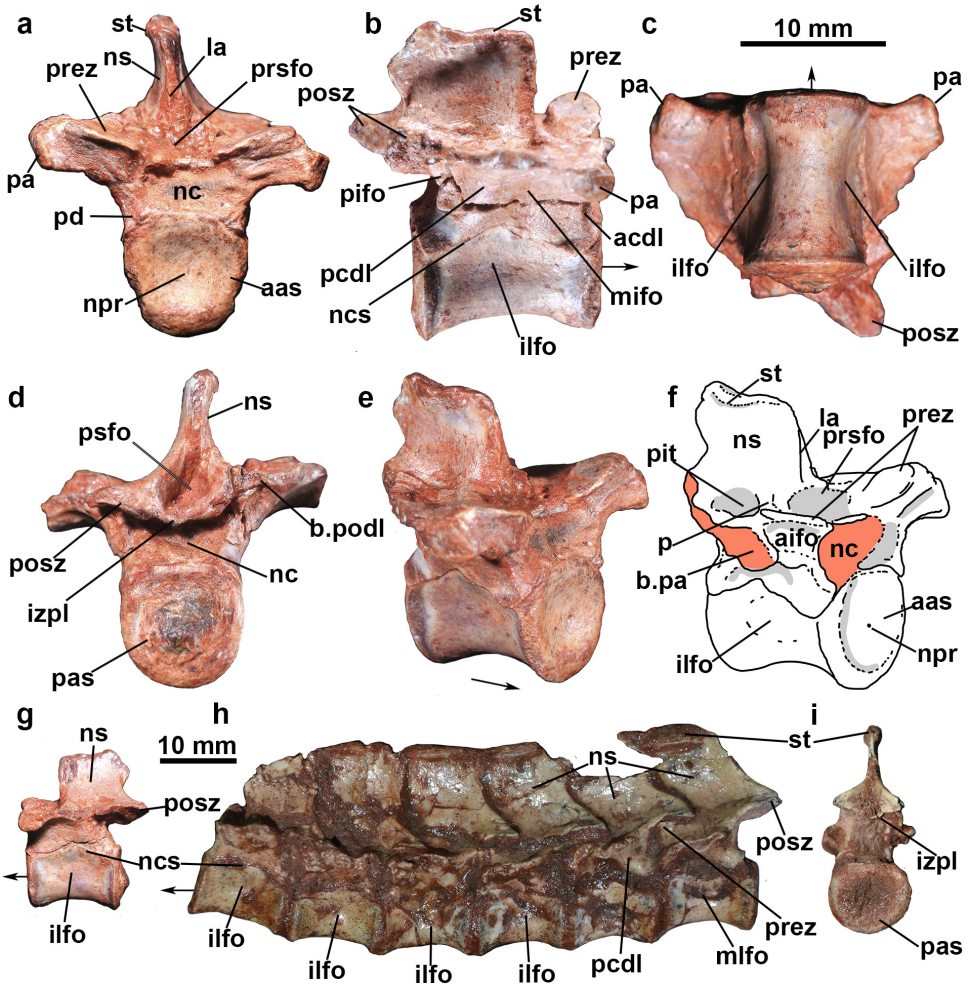

Figure 10. Details of the trunk vertebrae of *Polesinesuchus* (ULBRAPV003T) and a small-sized *Aetosauroides* specimen (MCP-13-PV). Trunk vertebrae of ULBRAPV003T in anterior (a), right lateral (b), ventral (c), posterior (d), anterolateral (e) and its interpretative drawing in anterolateral view (f). The same vertebra, viewed from the left lateral side (g), scaled with the trunk series of the specimen MCP-13-PV in lateral (h) and posterior view (i). Arrow indicates anterior direction. Abbreviations: aas, anterior articular surface; acdl, anterior centrodiapophyseal lamina; aifo, anterior infradiapophyseal fossae; b., broken; ilfo, incipient lateral fossae of the centrum; izpl, intrapostzygapophyseal lamina; la, lamina; mifo, middle infradiapophyseal fossa; nc, neural canal; ncs, neurocentral suture; ns, neural spine; npr, rudiments of the notochordal pit; p, pillar-like ridge; pa, parapophysis; pas, posterior articular surface; pcdl, posterior centrodiapophyseal lamina; pd, neural arch peduncle; pifo, posterior infradiapophyseal fossa; pit, deep pit lateral to the neural spine; prez, prezygapophyses; prsfo, prespinal fossa; psfo, postspinal fossa; podl, posterior zygodiapophyseal lamina; posz, postzygapophyses; st, spine-table.

Aetosauroides specimens (PVL 2073 and the large-sized PVL 2052; although the posterior extents of the lamina is missing). However, in MCP-3450-PV (Fig. 4e and 9b3: izpl) and other small-sized *Aetosauroides* specimens (MCP-13-PV, Fig. 10i: izpl) the intrapostzygapophyseal lamina is more straight and horizontal, resembling the condition of *Polesinesuchus* (ULBRAPV003T, Fig. 10d: izdl). The horizontal or the 'V-shaped' intrapostzygapophyseal lamina is not similar to the true hyposphene of *Desmatosuchus spurensis* (Parker 2008, see Stefanic & Nesbitt 2018), or to the posterior projection of *Scutarx* (Parker 2016b) and *Calyptosuchus* (Parker 2018a), or to the 'U- to Y-shaped' structure present in *Aetobarbakinoides* (CPEZ 168; Desojo et al. 2012, see Stefanic & Nesbitt 2018). The relationship of the intrapostzygapophyseal lamina and these other structures are yet unknown and future studies are needed to investigate that issue (see Gower & Schoch 2009, Parker 2016a).

In all available trunk vertebrae of UFSM 11070 (Fig. 5c and 6c: pit) and UFSM 11505 (Fig. 11d: pit), lateral to the base of the neural spine, a deep subcircular pocket pit (*sensu* Ezcurra 2016) is present which is identified here for the first time for *Aetosauroides*. In most vertebrae, it is possible to observe an anterior transverse ridge anteriorly limiting the pit (Fig. 5c and 6c: p). This ridge rises dorsally to the pit, also forming the posterolateral wall of the prespinal fossa (Fig. 6c: p) which is limited anteroventrally by a ventral bar (Fig. 5f: vb), similar to *Scutarx* (Parker 2016b). In the 10th posterior trunk vertebra of UFSM 11070, there is a pair of small foramina inside the anterior region of the pit (Fig. 6d). Pits

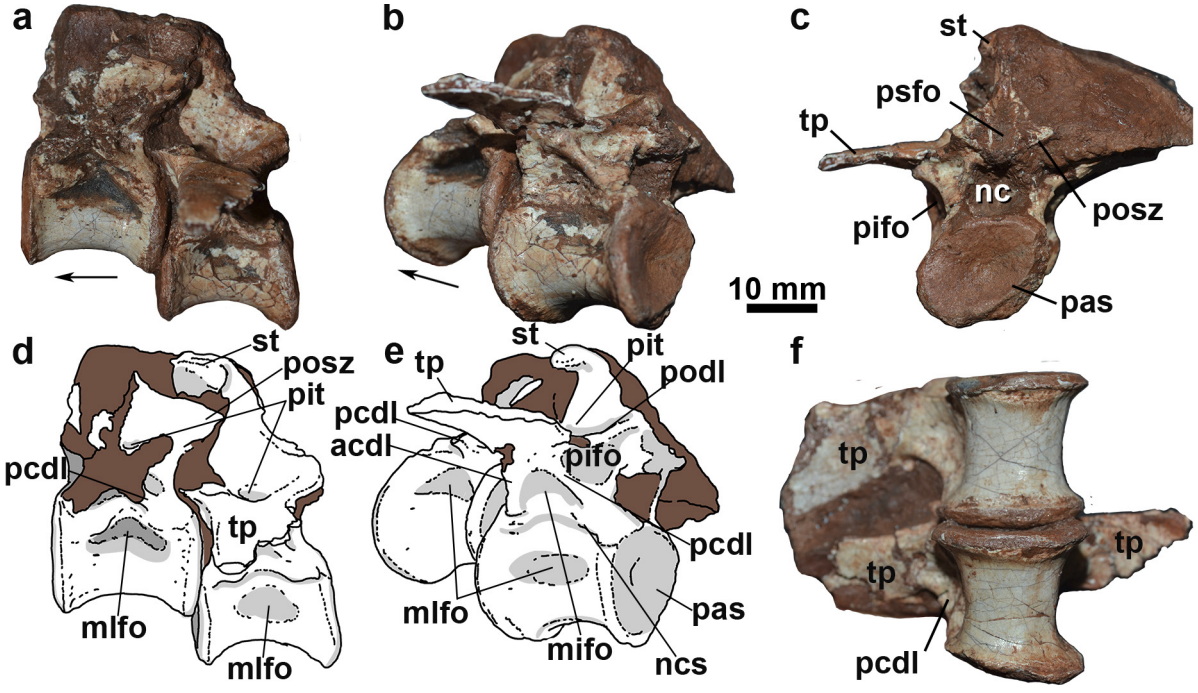

Figure 11. Posterior trunk vertebrae of *Aetosauroides* (UFSM 11505). In left lateral (a), posterolateral (b), posterior (c) and ventral (f) views. Interpretative drawings of the lateral (d) and posterolateral view (e). Arrow indicates anterior direction. Abbreviations: acdl, anterior centrodiapophyseal lamina; mifo, middle infradiapophyseal fossa; mlfo, wel-rimmed lateral fossae of the centrum; nc, neural canal; ncs, neurocentral suture; pas, posterior articular surface; pcdl, posterior centrodiapophyseal lamina; pifo, posterior infradiapophyseal fossa; pit, deep pocket pit lateral to the neural spine; psfo, postspinal fossa; podl, posterior zygodiapophyseal lamina; posz, postzygapophyses; st, spine-table; tp, transverse process.

lateral to the base of the neural spine are also observed in the trunk vertebrae of the small-sized MCP-3450-PV (Fig. 4d: pit), but they vary in depth and markedness within the series without apparent orientation. In the more anterior preserved neural arch, the anterior transversal ridge is marked (Fig. 4d: p), resulting in a deeper pit, although not as deep as in UFSM 11070 and UFSM 11505. However, just a depression is present in the anteriormost vertebrae of the articulated series (Fig. 8b: d), which is more marked in the subsequent vertebra (Fig. 8b: pit).

Remarkably, unlike what was stated by Roberto-da-Silva et al. (2014), the 13th (?) and 15th (?) vertebra of *Polesinesuchus* (ULBRAPV003T; Fig. 7 of Roberto-da-Silva et al. 2014) also present a shallow pit marked anteriorly by a pillar-like ridge (Fig. 10f: p and pit). Several aetosaurs present depressions lateral to the base of the neural spine, but no other aetosaur present deep subcircular pocket pits, with the exception of the sympatric *Aetobarbakinoides* (Desojo et al. 2012) and a single isolated aetosaur vertebra (NCSM 19672) from the Pekin Formation. A deep subcircular pit lateral to the base of the neural spine of the trunk vertebrae is shared with non-archosaur archosauriforms (see character 361 of Ezcurra 2016).

Spine tables are present in MCP-3450-PV (Fig. 9b2 and 9c: st), UFSM 11070 (Fig. 5a-d and 6a-c) and UFSM 11505 (Fig. 11: st) like other *Aetosauroides* (Casamiquela 1961, Desojo & Ezcurra 2011) and other aetosaurs (Desojo et al. 2013). However, their shape varies within and among the specimens. In the anterior trunk vertebrae of UFSM 11070, the spine table is less laterally expanded (Fig. 5a), being drop-shaped in dorsal view. The spine tables are heart-shaped (Fig. 5d and 6b), with a posterior pointed end, in the mid and posterior trunk series of UFSM 11070 and UFSM 11505. However, in the only available mid-trunk vertebra of MCP-3450-PV (Fig. 9b2 and 9c: st), the spine table is poorly laterally expanded, resembling the condition of other smaller specimens of *Aetosauroides* (MCP-13-PV; Desojo & Ezcurra 2011) and *Polesinesuchus* (Figure 7 of Roberto-da-Silva et al. 2014).

Desojo et al. (2012) have described the spine tables of the trunk vertebrae of the type material of *Aetosauroides* as being oval and of *Aetobarbakinoides* as being drop-shaped, although in both specimens the degree of preservation of these spine portions are questionable. Heart-shaped spine tables are present in the posterior trunk vertebrae of *Scutarx* (PEFO 34045), posterior trunk of cf. *Lucasuchus* (TMM 31185-65) and in some posterior trunk vertebrae of *Typothorax* (Martz 2002, TTU P-9214). Other aetosaurs, as noticed by other authors (e.g. Desojo et al. 2013), present different morphologies of the spine tables, like: squarer (anterior trunk vertebrae *Scutarx,* PEFO 34045; and *Paratypothorax* sp., TTU-P 9416), rectangular or hexagonal (*D. spurensis*, MNA V9300; Parker 2008) and rectangular with laterally compressed margins (isolated spine tables with this morphology in *Longosuchus*, TMM 31185-84).

As in other *Aetosauroides* specimens (Desojo & Ezcurra 2011), the anterior articular surfaces of the centra are almost as tall as wide in MCP-3450-PV, UFSM 11070 and UFSM 11505 (varying from 0.8 – 1), as in *Polesinesuchus* (0.8 – 1) and *Aetobarbakinoides* (0.87 – 1.1), but their posterior surfaces is slightly wider than tall. In some vertebrae of the small-sized MCP-3450-PV, it is possible to observe the remnants of the notochordal pit in the posterior articular surfaces (Fig. 9f3 and 9g3: np). In the type material of *Polesinesuchus*, although not marked, a small pit with distinct color is present in the posterior articular surface of the trunk centra and in some anterior surfaces (Fig. 10a: npr), and may also represent a remnant of the

notochordal pit, but it is not as deep or large as in MCP-3450-PV. Also, as observed by Desojo & Ezcurra (2011) for MCP-13-PV and PVL 2073, most trunk vertebrae of UFSM 11070 (Fig. 7b4: fs) and MCP-3450-PV (Fig. 8c, 9b5, 9d2, 9e2 and 9f4: fs), present flat surfaces. Nevertheless, some more posterior trunk vertebrae presents more convex surfaces in MCP-3450-PV (Fig. 9g4) and in UFSM 11505 (Fig. 11f).

Well-rimmed lateral fossae, ventral to the neurocentral suture, are present in the posterior trunk centra of UFSM 11070 (Fig. 7b3: mlfo) and UFSM 11505 (Fig. 11d and 11e: mlfo), representing an important autapomorphy of *Aetosauroides* (Desojo & Ezcurra 2011). However, in the mid-trunk of UFSM 11070 (Fig. 7a: ilfo) and in all available trunk centra of the small-sized MCP-3450-PV (Fig. 4h, 4i, 8e, 9b3, 9d1, 9e1, 9f2 and 9g2: ilfo), this feature is not evident or excavated as in those specimens, being just a shallow elliptical fossa or depression. This condition resembles the one found most vertebrae of the small-sized MCP-13-PV (Fig. 10h: ilfo), which is just slightly more marked than the incipient lateral fossae of the trunk centra present in *Polesinesuchus* (Fig. 10b, 10c, 10f and 10g: ilfo; unlike sated by Roberto-da-Silva et al. 2014). The incipient fossa of the posterior trunk of small-sized specimens, contrasts with those of larger Argentine (PVL 2073 and PVL 2052) and of the Brazilian (e.g. UFSM 11070 and UFSM 11505) *Aetosauroides* specimens. This indicates that this character is not only variable within the axial series, but also between individuals of different sizes and ontogenetic stages (see Discussion).

Sacral vertebrae

In UFSM 11070 two sacral vertebrae (Fig. 12) are present, as in other aetosaurs (Walker 1961, Casamiquela 1961, 1967, Desojo & Báez 2005, Parker 2008, Roberto-da-Silva et al. 2014, Parker 2018a). Although covered by osteoderms, it is possible to indicate that their neural arches were not fused and that the neurocentral suture is opened (Fig. 12b). However, the sacral ribs are fused to each other, by a distal expansion of the second sacral rib (Fig. 12d: aesr). This condition is shared with other aetosaurs, like *Stagonolepis robertsoni* (Walker 1961), *Desmatosuchus spurensis* (Parker 2008) and apparently in other *Aetosauroides* (PVL 2052 and PVL 2073). Only the anterior articular surface of the first sacral vertebra is visible in UFSM 11070, being sub-circular in morphology. However, an isolated second sacral centra of the small-sized specimen UFRGS-PV-1514-T (Fig. 13a1 and 13a2: aas) is preserved, being dorsoventrally constricted and with a flat surface (Fig. 13a2) typical of other aetosaurs (Parker 2008). The articular surfaces are elliptical, being wider than tall (Fig. 13a1), a condition less marked in *Polesinesuchus*. In UFRGS-PV-1514-T, the sacral vertebrae centra are not fused to each other as other *Aetosauroides* (e.g. PVL 2073 and PVL 2052), although unknown in UFSM 11070. Conversely, the sacral vertebrae are fused between each other and with the last trunk vertebra in *Desmatosuchus spurensis* and *Longosuchus meadei* (Parker 2008, 2016a).

Caudal vertebrae

The anterior caudal series are preserved in articulation in in UFRGS-PV-1514-T (Fig. 13c1 and 13c2; only the centra in the latter specimen) and UFSM 11070 (Fig. 14a), with the neurocentral suture open in both specimens. Three anterior caudal vertebrae of UFSM 11505 (Fig. 15a and 15b) and two small mid-caudal vertebrae putatively referred to the small-sized MCP-3450-PV (Fig. 15c2) have closed neurocentral sutures. More than 10 posterior caudal vertebrae were found isolated, keeping us from confidently attributing them to other specimens. Some of these

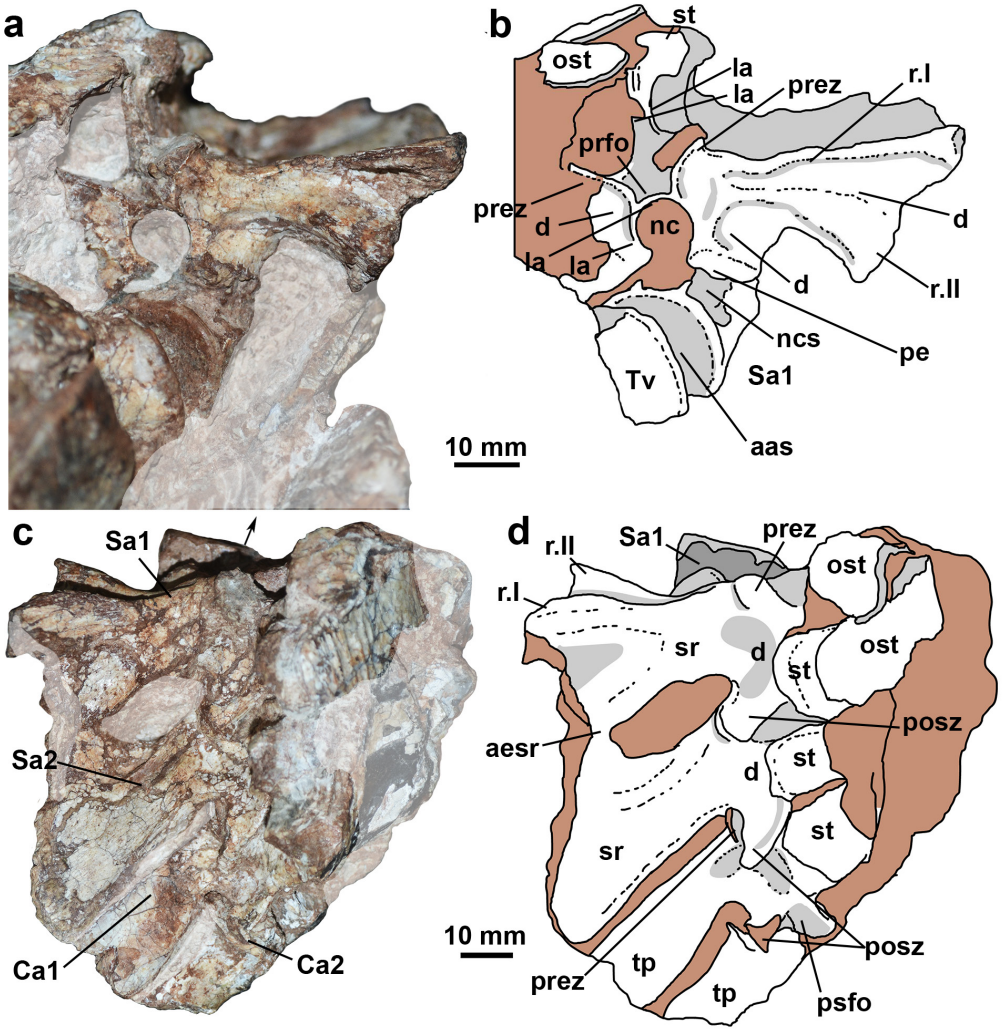

Figure 12. Sacral vertebrae of *Aetosauroides* (UFSM 11070). a, first sacral vertebra in anterior view. b, both sacrals and first caudals in dorsal view. Interpretative drawings of the anterior (b) and dorsal views (d). Arrow indicates anterior direction. Abbreviations: aas, anterior articular surface; aesr, anterior expansion of the sacral rib - being confluent with the first sacral rib; Ca, caudal vertebra; d, depression; la, lamina; nc, neural canal; ncs, neurocentral suture; ost, paramedian osteoderm fragment; prez, prezygapophyses; prsfo, prespinal fossa; psfo, postspinal fossa; posz, postzygapophyses; r.I, ridge I; r.II, ridge II; Sa, sacral vertebra; sr, sacral rib; st, spine-table; tp, transverse process; Tv, trunk vertebra.

represent more distal vertebrae and also have closed neurocentral sutures.

The two anterior caudals of UFSM 11070 are as tall as the sacral vertebrae. The neural spine is shorter than the transverse process in the anterior caudals, bearing a spine table (Fig. 12d and 14e: st). The spine tables are lateromedially expanded and rectangular in dorsal view (slightly wider than long) in the anterior caudals (Fig. 12d: st), resembling those of the sacrals. The spine table of the fifth caudal is more heart-shaped (Fig. 14e: st), resembling the morphology of the trunk series. Remarkably, spine tables are absent in the putative anterior caudal vertebrae of the small-sized MCP-3450-PV, suggesting intraspecific variation. The postzygapophyses of

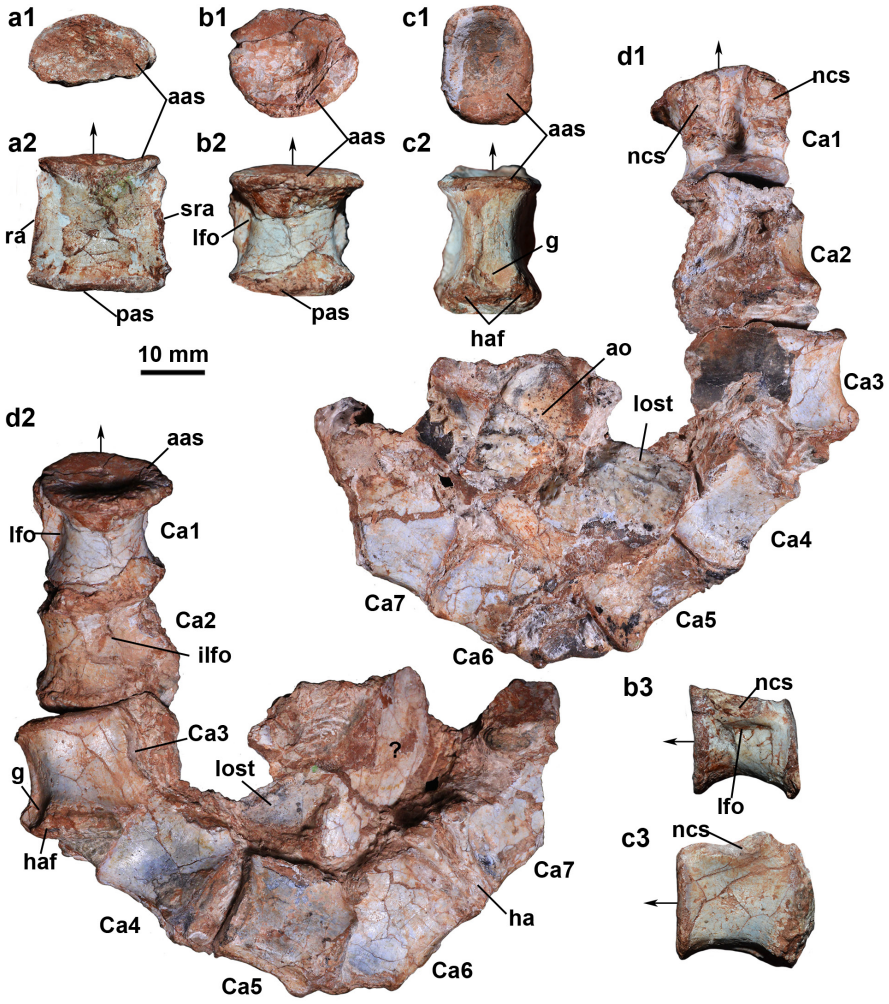

Figure 13. Sacral and caudal centra of *Aetosauroides* (UFRGS-PV-1514-T). a, second sacral centrum in anterior (a1) and ventral (a2) views. b, first caudal in anterior (b1), ventral (b2) and lateral (b3) views. c, third caudal in anterior (c1), ventral (c2) and lateral (c3) views. d, preserved articulated centra of the caudal series in dorsal (d1) and ventro-lateral view (d2). Arrow indicates anterior direction. Abbreviations: aas, anterior articular surface; ao, appendicular osteoderm; Ca, caudal vertebra; g, groove; ha, hemal arch; haf, hemal arch facet; ilfo, incipient lateral fossae of the centrum; la, lamina; lfo, lateral fossa; lost, lateral osteoderm; ncs, neurocentral suture; pas, posterior articular surface; sra, articular facet for the sacral rib.

UFSM 11070 (Fig. 14c and 14e: alp), and UFSM 11505 (Fig. 15a2: alp), bear spinoposzygapophyseal laminae which have a convex expansion, resembling an aliform process as in titanosaur dinosaurs (e.g. Salgado & Powell 2010).

A prominent lateral fossa, ventral to the neurocentral suture, is present in the anteriormost caudal vertebrae of UFSM 11070 (Fig. 14a: lfo) and UFRGS-1514-T (Fig. 13b3: lfo), contrasting with the almost flat lateral surface of the centra of more posterior caudals of these specimens (Fig. 13c3, 14f) and UFSM 11505 (Fig. 15a1 and 15b1). Interestingly, in distalmost caudal vertebrae of UFSM 11070 a slight lateral fossa is present ventral to the neurocentral suture region (Fig. 15j5 and 15k1: slfo). In other aetosaurs, just depressions are present in the anterior caudal vertebrae (e.g. *S. robertsoni*, NSM R-4787; and *Typothorax,* MCZ 1488; Martz 2002), but marked fossae of the more anterior caudal series is only shared with *Aetosauroides* (PVL 2073 and PVL 2052), which indicate the small-sized UFRGS-1514-PV is probably an *Aetosauroides* specimen.

The hemal arch facets in UFSM 11070, which preserves a complete anterior caudal sequence, are present from the fourth vertebra until the more posterior caudal centra (Fig. 14a: haf). The hemal arch in UFRGS-PV1514-T is present at the third available caudal (Fig. 13c2: haf). This condition contrasts with that of the type material of *Aetosauroides* (PVL 2073) in which the first hemal arch facet is placed at the second

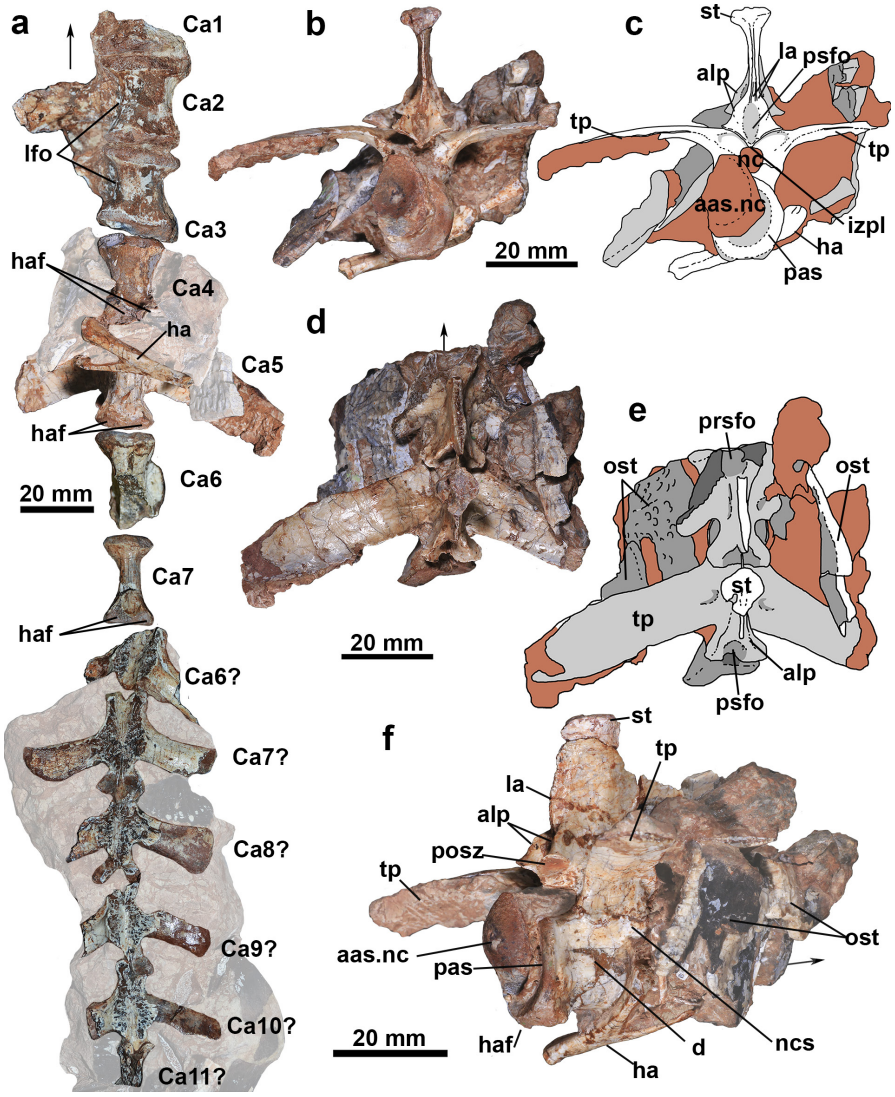

Figure 14. Caudal vertebrae of *Aetosauroides* (UFSM 11070). a, sequence of available caudal vertebrae in ventral view, with the six first ones found in articulation. Details of the fifth caudal vertebra in posterior (b), dorsal (d) and posterolateral view (f) and interpretative drawings in posterior (c) and dorsal views (e). Arrow indicates anterior direction. Abbreviations: aas.nc, anterior articular surface natural cast; alp, aliform-like process; d, depression; Ca, caudal vertebra; ha, hemal arch; haf, hemal arch facet; izpl, intrapostzygapophyseal lamina; la, lamina; lfo, lateral fossa; nc, neural canal; ncs, neurocentral suture; ns, neural spine; ost, paramedian osteoderm fragment; pas, posterior articular surface; prsfo, prespinal fossa; psfo, postspinal fossa; posz, postzygapophyses; psfo, post-spinal fossa; st, spine-table; tp, transverse process.

caudal centra. Remarkably, a probable dimorphic condition occurs in *S. robertsoni*, in which the hemal facets start either at the second or at the fifth caudal vertebrae which may be related to sexual dimorphism (Walker 1961).

Paramedian osteoderm bone histology of *Polesinesuchus*

In order to evaluate the effect of the ontogeny in *Aetosauroides* taxonomy and its implications of Brazillian aetosaur diversity, we provide a brief analysis of the microstructure of a parasagittal slice of a paramedian osteoderm of the type material of *Polesinesuchus*, probably from the anterior caudal region (Fig. 16a and 16e). As in other aetosaurs (Cerda & Desojo 2011, Scheyer et al. 2014) three distinct regions can be observed: external, internal and basal (Fig. 16a). The external layer (Fig. 16b1: el) is composed of lamellar zonal bone tissue, mostly avascular, as in other aetosaurs (Cerda et al. 2018). This layer (16b1: lb) forms the osteoderm's external ornamentation (Scheyer et al. 2014, Cerda et al. 2018). As the pits and grooves which compose the ornamentation of the external surface are not expressive in *Polesinesuchus*, reflecting a lower amount of cycles of bone erosion and deposition (Fig. 16a and b). However, some

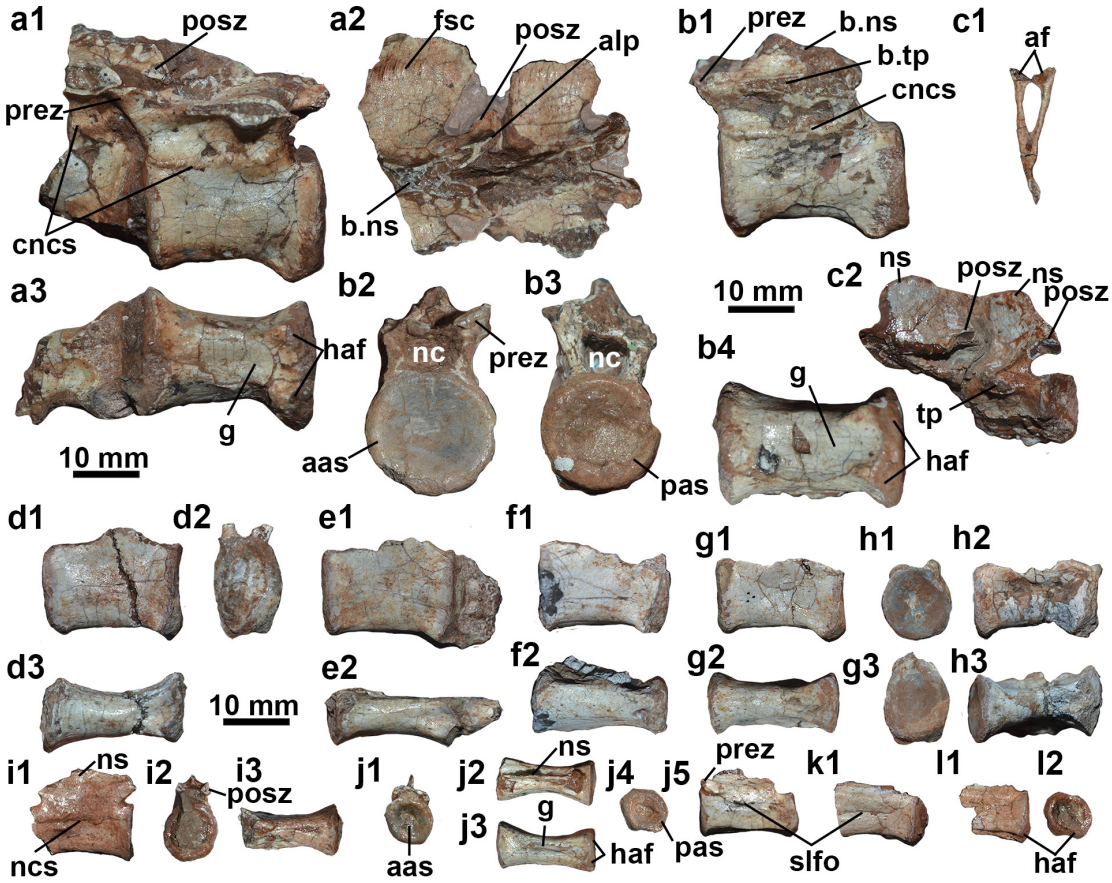

Figure 15. Posterior caudals and hemal arches of *Aetosauroides* (MCP-3450-PV, UFSM 11070 and UFSM 11505). a, two articulated caudals of UFSM 11505 in lateral (a1), dorsal (a2) and ventral (a3) views. b, an isolated caudal of UFSM 11505 in lateral (b1), anterior (b2), posterior (b3) and ventral (b4) views. c1, isolated hemal arch of MCP-3450-PV, in anterior view. c2, articulated caudal vertebrae of MCP-3450-PV. Ten isolated caudal vertebrae of UFSM 11070 and probably some of MCP-3450-PV or UFRGS-1514-T in lateral (d1-l1), anterior (h1-j1), ventral (d3-j3), posterior (d2, g3, i2, j4 and l2) and dorsal views (j2). Abbreviations: aas, anterior articular surface; af, articular facets; alp, aliform-like process; b., broken; cncs, closed neurocentral suture; fsc, fusion scar; g, groove; ha, hemal arch; haf, hemal arch facet; nc, neural canal; ncs, neurocentral suture; ns, neural spine; pas, posterior articular surface; prez, prezygapophyses; posz, postzygapophyses; slfo, slit-like lateral fossae of the centrum; tp, transverse process.

cycles of bone deposition and resorption lines showing erosion are present in a pit (Fig. 16d1: rl), as well as resorption bays (Fig. 16b1: rb). Several osteocyte lacunae are globular at the external layer (Fig. 16d1: gol), with some branching canaliculi. The osteocyte lacunae density in the external cortex is relatively lower relative to the internal layer, as in *Aetosauroides* (Cerda & Desojo 2011). Contrasting from *Aetosauroides* (Cerda et al. 2018), no Sharpey's fibers were observed in the external cortex.

The transitional zone between the external and the internal layer shows several vascular channels and some primary osteons (Fig. 16b1 and 16d2: po); there is no resorption separating the external and the internal cortex as was observed by Cerda et al. (2018) for *Aetosauroides*, but secondary reconstruction is present in this transitional area (Fig. 16a), ventral to the

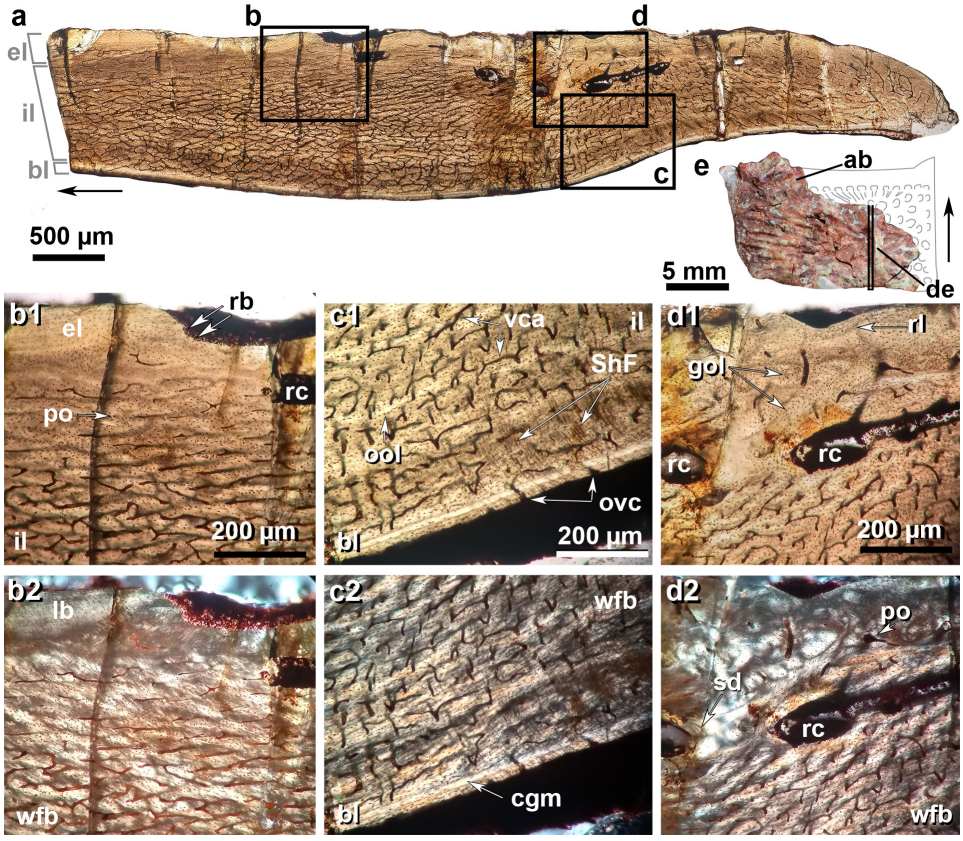

Figure 16. Osteoderm paleohistological thin-section of the holotype of *Polesinesuchus aurelioi*. a, Composite image of the paramedian dorsal trunk osteoderm (arrows indicate anterior region). b, external and internal cortex details in conventional light (b1) and polarized light (b2), showing the external erosion by the resorption bays and the internal cortex vascularization pattern, with some primary osteons. c, internal cortex and basal layer detail in conventional light (c1) and polarized light (c2) showing the Sharpey fibers orientation and the cyclical growth mark. d, external layer and internal cortex detail the globular osteocyte lacunae, primary osteons and the resorption cavities evidencing the secondary remodeling in conventional light (d1) and polarized light (d2). e, dorsal view of sectioned osteoderm, showing the targeted slice. Abbreviations: bl, basal layer; cgm, cyclical growth mark; el, external layer; gol, globular osteocyte lacunae; il, inner layer; lb, lamellar bone; ool, organized distribution of osteocyte lacunae; ovc, open vascular channels; po, primary osteon; rb, resorbtion bays; rc, resorbtion cavities, rl, resorption line; ShF, Sharpey fibers; sd, secondary deposition; vca, vascular channels anastomoses; wfb, woven fibered bone.

dorsal eminence region represented by large resorption cavities (Fig. 16d: rc). Few cavities present deposition of lamellar bone layers (Fig. 16d2: sd), which indicate a single remodeling event. This moderate secondary remodeling ventral to the dorsal eminence is shared with other *Aetosauroides* specimens (Cerda & Desojo 2011, Cerda et al. 2018), but contrasts with the high secondary remodeling observed in most aetosaurs, including *Paratypothorax, Calyptosuchus* and *Stagonolepis olenkae* (see Scheyer et al. 2014).

The inner cortex is composed of highly vascularized woven-fibered bone with disorganized collagen fibers (Fig. 16b2 and c2: wfb). Small amounts of incipient fibro-lamellar complex are observed (Fig. 16d2), resembling the condition in *Aetosauroides* (Cerda et al. 2018). The vascular channels radiate from the upper center (ventral to the dorsal eminence area) toward all portions of the osteoderm (Fig. 16a).

These vascular channels are usually parallel to the external surface, with irregular anastomoses in the posterior and anterior areas of the inner cortex (Fig. 16c1: vca) forming a reticulate pattern. Similar to smallest specimen known of *Aetosauroides* MCP-13 (Cerda & Desojo 2011) there are few primary osteons. Both globular and flattened osteocyte lacunae are present in this tissue, distributed irregularly, except in the ventral portion, where some flattened lacunae are organized in parallel rows (Fig. 16c1: ool).

The basal cortex is relatively thin when compared with sampled *Aetosauroides* specimens (Cerda & Desojo 2011, Cerda et al. 2018). This condition differs from the model of Cerda et al. (2018), in which the basal cortex is expected to be larger in immature individuals. It is composed of a parallel-fibered bone tissue (but see Cerda et al. 2018), without marked vascularization, although in the ventral portion parallel vascular channels (Fig. 16c1: ovc) with some anastomoses with vascular channels at the inner layer can be observed. These vascular channels are transversally oriented in relation to the osteoderm. The osteocyte lacunae are mainly flat (as occurs in *Aetosauroides* PVL 2073, Cerda et al. 2018), but scattered globular ones can also be observed. The limits between the basal cortex and the inner layer are not as well marked as in *Aetosauroides* (PVL 2073 and PVL 2052, Cerda et al. 2018). A single distinct cyclical growth mark can be observed (Fig. 16c2: cgm). The inside of this growth mark is poorly vascularized, the osteocyte lacunae are flattened, and their density is low compared with the basalmost region. We interpret it as an annulus, which is commonly found in immature aetosaurs (see Cerda et al. 2018). Different from a line of arrested growth, the annulus signalizes a reduction in the growth of the osteoderm (Francillon-Vieillot et al. 1990).

DISCUSSION

Intraspecific variation of the axial skeleton

Our results reveal further details on the axial osteology of *Aetosauroides* as well as elucidate some misunderstood post-cranial characters of *Polesinesuchus*. We have documented intraspecific variation in the axial skeleton of *Aetosauroides* specimens, including some diagnostic features in the trunk series (*sensu* Casamiquela 1961, 1967, Desojo & Ezcurra 2011) used in broader scope archosaur phylogenies (e.g. Nesbitt 2011, Ezcurra 2016, Ezcurra et al. 2017, Nesbitt et al. 2018; see item 5 of the Supplementary material). This includes: (i) incipient or well-rimmed lateral fossae ventral to neurocentral suture; (ii) the centrodiapophyseal lamina incipient and pillar-shaped or pronounced; and (iii) a depression or a deep pit lateral to the neural spine. These variable features are discussed below:

Lateral fossae

Lateral fossae on vertebral centra are interpreted as places for fat deposits in extant and extinct pseudosuchians (Wedel 2003, O'Connor 2006, Butler et al. 2012), which may increase in size throughout the individual's lifetime based on phytosaurs (Irmis 2007). As identified in our study, small-sized and probably immature *Aetosauroides* specimens (MCP-13-PV and MCP-3450-PV) present incipient lateral fossae or depressions along their trunk series, being considerably less developed when compared with those present in UFSM 11505, UFSM 11070 and the type material PVL 2073. The condition observed in MCP-13-PV and MCP-3450-PV is similar to that of *Polesinesuchus* (unlike stated by Roberto-da-Silva et al. 2014), although some centra of MCP-13-PV may appear more marked because of the collapse of the inner bone wall (like in the fourth and fifth vertebrae, Fig. 10h).

A slight lateral depression is present in most other aetosaurs vertebral centra (e.g. Desojo & Ezcurra 2011), like in *S. robertsoni* (NMS R4796 and NMS R4799), *Scutarx* (PEFO 34045, Parker 2016b), *C. chathamensis* (NCSM 23618) and *Tecovasuchus* (TTU P0545, Martz & Small 2006). More importantly, no fossa or depression is observed on the lateral surface of the centra of *Aetobarbakinoides*, which indicate its taxonomic validity among other characteristics, as it is similar in size to the type material of *Aetosauroides* (PVL 2073), UFSM 11505 and UFSM 11070. The clear absence of depressions on the trunk vertebrae of *Aetobarbakinoides* is shared with *Calyptosuchus* (UCMP 78708), *Longosuchus* (TMM 31185-84), c.f. *Lucasuchus* (TMM 31100-448; TMM 31185-65), *D. spurensis* (MNA V9300) and *D. smalli* (TTU-P 9416) and in most vertebrae of *Stagonolepis olenkae* (e.g. ZPAL AbIII 3317).

Centrodiapophyseal laminae and the infradiapophyseal fossae

The conspicuousness of these structures differs between individuals of *Aetosauroides*. Although Desojo & Ezcurra (2011) have identified variation in the presence of the anterior infradiapophyseal fossa in *Aetosauroides*, the available sample turns possible to observe variation also in the laminae morphology. Small and immature specimens have incipient pillar-like lamina (MCP-13-PV and MCP-3450-PV), like those found in *Polesinesuchus* (ULBRAPV003T), whereas, in contrast, more mature specimens present pronounced pillar-like laminae (PVL 2059, PVL 2073 and UFSM 11070) or thinner and clearly defined laminae (UFSM 11505, PVL 2073 and in the large-sized PVL 2052). Additionally, as noticed for MCP-13-PV (Desojo & Ezcurra 2011) some variation within the series of a single specimen also occurs. In the anterior trunk sequence of PVL 2073, UFSM 11070 and MCP-3450-PV the anterior lamina is generally poorly developed and the posterior lamina is more prominent and pillar-like (incipient in MCP-3450-PV). Nevertheless, in posterior trunk vertebrae of PVL 2073 and UFSM 11070 more prominent and thinner anterior and posterior laminae are present.

The centrodiapophyseal laminae are present in most other aetosaurs (e.g. Desojo & Báez 2005, Parker 2008) but their morphology varies. Pillar-like laminae are present in most mid and large-sized stagonolepidoidean aetosaurs, like *Desmatosuchus* (*D. spurensis*, MNA V9300; *D. smalli*, TTU-P 9416), *Calyptosuchus* (UCMP 78708), *Stagonolepis robertsoni* (NMS R-4796) and *S. olenkae* (ZPAL AbIII 3317). However, a sharp and thin lamina is present in *Lucasuchus* (TMM 31100-452 and TMM 31100-448) and *Longosuchus* (TMM 31185-84). Also, no lamina appears to present in *Neoaetosauroides* (Desojo & Ezcurra 2011), which may be an autapomorphic condition in that taxon. Remarkably, in some trunk vertebrae of *Typothorax* (e.g. Martz 2002), *Longosuchus* (TMM 31185-84), *D. spurensis* (MNA V9300; Parker 2008), *D. smalli* (TTU-P 9416), *Calyptosuchus* (Parker 2018a) and *Scutarx* (PEFO 34045), the anterior and posterior centrodiapophyseal laminae are joined together dorsally, as one centrodiapophyseal pillar-like lamina (ventral strut of Parker 2018a), which may continue to the base of the transverse process. Further studies are needed to understand the ontogenetic or phylogenetic signal of these structures within Aetosauria.

Deep pocket pits lateral to the neural spine

This feature is observed for the first time in *Aetosauroides* and in *Polesinesuchus*, although less marked in the latter. In MCP-3450-PV, a small-sized individual of *Aetosauroides*, the pit is poorly marked in some mid-trunk vertebrae, being more developed in the anteriormost

and more posterior trunk vertebrae. A larger, deeper and more elliptical pit is present in all of the trunk vertebrae of UFSM 11070 and in the available trunk vertebrae of UFSM 11505. Still, the presence of this feature in the Argentine *Aetosauroides* sample is unknown because a thick encrustation covers most of the vertebra in the *Aetosauroides* type material and in addition to the damage done by the original over preparation that removed many features.

The presence of a deep subcircular pit lateral to the neural spine in mature *Aetosauroides* is only shared with the sympatric *Aetobarbakinoides* and with an isolated vertebra from the Pekin Formation (cf. *Coahomasuchus chathamensis*). In most aetosaurs only a shallow depression is present lateral to the neural spine, like in *Scutarx* (PEFO 34045), *S. robertsoni* (at least in the anterior trunk vertebrae, NMS R-4796), *S. olenkae* (ZPAL AbIII 3177) and in *Paratypothorax* sp. (at least in the posterior trunk vertebrae TTU-P 9416). However, no depression or pit is observed in *Calyptosuchus* (UCMP 78708), *D. spurensis* (MNA V9300), *D. smalli* (TTU-P 9416), c.f. *Lucasuchus* (TMM 31185-65), *Longosuchus* (TMM 31185-84) and in *Typothorax* (PEFO 33967, considering that this specimen preserves mid-trunk vertebrae; and MCZ 1488, which presents a badly preserves posterior trunk vertebrae).

Beside the characters discussed above, the spine table morphology and the shape of the intrapostzygapophyseal lamina also vary in the present sample. Poorly expanded triangular spine tables are present in the small-sized MCP-3450-PV, like in the similarly small MCP-13-PV specimen (Desojo & Ezcurra 2011) and *Polesinesuchus* (Roberto-da-Silva et al. 2014). This contrasts with the well expanded spine tables (cordiform or oval) of larger individuals (UFSM 11070, UFSM 11505, PVL 2073 and in the large-sized PVL 2052). The intrapostzygapophyseal lamina also appears to be horizontal in smaller *Aetosauroides* (MCP-13 and MCP-3450-PV), like in *Polesinesuchus*, but is 'V-shaped' in more mature specimens (UFSM 11070 and PVL 2073). The presence of a horizontal or 'V-shaped' intrapostzygapophyseal laminae in *Aetosauroides* differs them from the 'U-shaped' lamina or the 'hyposphene' structure of Desojo et al. (2012, see Stefanic & Nesbitt 2018) of *Aetobarbakinoides*. There is no indication that the 'V-' or the 'U-' shaped intrapostzygapophyseal lamina are ontogenetic precursors of the hyposphene accessory articulation found in other aetosaurs (see Parker 2016a,b, Stefanic & Nesbitt 2019), which it is also absent in more mature specimens of *Aetosauroides* (PVL 2052 sensu Taborda et al. 2013, Cerda et al. 2018).

Body size and ontogeny of *Aetosauroides*

Recent studies have improved our understanding of the maturity and sexual dimorphism of *Aetosauroides* individuals (Cerda & Desojo 2011, Taborda et al. 2013, 2015, Cerda et al. 2018). Histological thin-sections of paramedian osteoderms provide a good record of lines of arrested growth (LAG) count in *Aetosauroides* (e.g. Cerda & Desojo 2011, Cerda et al. 2018), indicating that individuals larger than one meter were probably sexually mature but not fully grown (Taborda et al. 2013, Taborda et al. 2015, Cerda et al. 2018). This also applies to the type material of *Aetobarbakinoides*, which appear to be about 10 years old at least at the time of death (*sensu* Cerda et al. 2018). Taborda et al. (2015) have also indicated that age and body length were not well correlated in *Aetosauroides*, as similarly sized specimens (PVL 2073 and PVL 2059) have different LAG counts (5 and 10, respectively) in their osteoderms, besides differences in osteoderm ornamentation, suggesting sexual dimorphism as one of the potential reasons for this variation. To those authors, males

could achieve more than two meters in length, whereas females would be usually smaller than 1.5 meters.

Skeletal maturity is also corroborated by the degree of neurocentral suture closure (see Brochu 1992, 1996, Irmis 2007, Ikejiri 2012, Taborda et al. 2015). The small size specimen UFRGS-PV-1514-T does not preserve an osteoderm LAG count, as it is represented solely by a caudal series with opened neurocentral sutures, thus indicating it was skeletally immature. The specimen UFSM 11070, comparable in body size to *Aetosauroides* type material PVL 2073, presents 8 LAGs (according to Cerda & Desojo 2011, Taborda et al. 2013, 2015) and its trunk and anterior caudals have open neurocentral sutures, being considered, as in PVL 2073, an sexually mature male specimen (Taborda et al. 2013, 2015). However, the similarly sized specimen UFSM 11505 presents closed neurocentral sutures in the anterior caudals, that are also closed in the putative anterior caudals referred to MCP-3450-PV, which was probably smaller than one meter of total length based on vertebrae size. As there is no LAG information available for both specimens, we indicate tentatively that these specimens may represent females, respectively being probably sexually mature (UFSM 11505) and immature (MCP-3450-PV). It is interesting that some of these specimens were found in close association, resembling other known juvenile aetosaur accumulations (Schoch 2007). Specimen MCN-PV 2347 does not preserve caudal vertebrae or any osteoderm LAG count. No histological analysis was performed on the type material of *Polesinesuchus* until the present study.

Revision of the taxonomic status of *Polesinesuchus* and *Aetobarbakinoides*

These variable features (i.e. centrodiapophyseal laminae and fossae; deep pocket pit; and well-rimmed lateral fossae) were described as absent by Roberto-da-Silva et al. (2014) for the small-sized *Polesinesuchus* type specimen. However, they are simply not as evident in *Polesinesuchus* as they are in more larger sized *Aetosauroides*, resembling the condition of small and immature *Aetosauroides* specimens (MCP-13-PV *sensu* Cerda & Desojo 2011, Taborda et al. 2013, 2015, and MCP-3450-PV, this study). To scale up these individuals we plotted their centrum length (Table I) against the minimum femur circumference (see item 3 of Supplementary Appendix and Fig. S3). Based on trunk vertebrae length, the smallest known *Aetosauroides* (MCP-13-PV) is similar in size to *Polesinesuchus*, with MCP-3450-PV being an intermediate between those two specimens and larger *Aetosauroides* specimens (PVL 2059, PVL 2073, UFSM 11070, UFSM 11505 and PVL 2052). Remarkably, the longest trunk centra of *Aetobarbakinoides* is slightly larger than those of UFSM 11070 and PVL 2073, although its femur circumference is smaller.

The immature ontogenetic stage of the type material of *Polesinesuchus* was originally indicated by Roberto-da-Silva et al. (2014), as its entire axial series with opened neurocentral sutures, including the posteriormost available caudal vertebrae. The paramedian osteoderm histology of *Polesinesuchus* performed by our study supports that the type material ULBRAPV003T was indeed an immature, based on: (1) the high degree of vascularization of the basal layer (see Cerda et al. 2018); and (2) the presence of only one cyclical growth mark (annulus); (3) the majority predominance of fast growing woven bone in the inner layer. We can thus estimate that the type specimen was at least two years old (based on Cerda & Desojo 2011, Taborda et al. 2013) and with a total length of about 0.76 meters at the time of death (measurement using the femur length; see Taborda et al. 2013). This is similar to the estimated age of MCP-13-PV

Table I. Comparative matrix of *Aetosauroides* (MCP-3450-PV, MCP-13-PV, PVL 2059, PVL 2073, PVL 2052, UFSM 11070 and UFSM 11505), '*Polesinesuchus*' (ULBRAPV003T) and *Aetobarbakinoides* (CPEZ 168) axial features. *Aetosauroides* specimens without available trunk vertebrae (MCN 2347, PVL 2091 and UFRGS-PV-1514-T) were excluded. Cyclical growth mark (CGM) count and total length for *Aetosauroides* and *Aetobarbakinoides* is provided by Cerda & Desojo (2011), Taborda et al. (2013; 2015) and Cerda et al. (2018). CGM count and total length of '*Polesinesuchus*' is provided by this study.

SPECIMEN	ULBRAPV003T	MCP-13-PV	MCP-3450-PV	PVL 2059	PVL 2073	UFSM 11070	UFSM 11505	PVL 2052	CPEZ 168
Estimated total length (m)	0.74	~0.8	~1	1.3	1.39	1.34	1.45	2.42	~1.3
Femur circumference	33	-	-	-	59.5	57.6	63.3	104.4	41.3
Large trunk vertebra length (mm)	13.9	13.3	17.2	24.2	25.7	25.7	22.3	~37	29.3
Anteriormost closed neurocentral suture	0*	PCA	ACA*	CE	PCA	PCA	ACA	PTV*	ATV
CGM count	1	-	-	10	5	8	5	21	-
PTV, presence of *acdl*: (0) incipient; (1) marked.	0	0	0	0	1	1	1	1	A
PTV, presence of *pcdl*: (0) incipient; (1) marked.	0	0	0	1	1	1	1	1	1
ATV, lateral fossae: (0) depression; (1) well-rimmed.	0	-	0	0	1	-	-	-	a
PTV, lateral fossae: (0) depression; (1) well-rimmed fossa.	0	0	0	1	1	1	1	1	a
Spine table: (0) non-expanded; (1) drop, oval or cordiform.	0	0	0	-	1	1	1	1	1
Lateral to the neural spine: (0) depression; (1) deep pocket.	0	-	0	-	-	1	1	-	1
Intrapostzygapophysial lamina: (0) horizontal; (1) V-shaped; (2) U-shaped.	0	0	0	-	1	1	1	1	2

***Based on available vertebrae. Abbreviations: a, absent; acdl, anterior centrodiapophysial lamina; ATV, anterior trunk vertebrae; ACA, anterior or mid-caudal vertebra; CE, cervical vertebra; PCA, posterior caudal vertebrae; pcdl, posterior centrodiapophysial lamina; PTV, posterior trunk vertebrae.**

(Taborda et al. 2013, Cerda & Desojo 2011) a small *Aetosauroides* specimen of almost equivalent size to *Polesinesuchus* (Desojo & Ezcurra 2011). However, the size of *Polesinesuchus* is larger than the 0.39 meters estimated by Cerda et al. (2018) for the two years old PVL 2073, which used retro-calculation method of osteoderm-thin sections.

Polesinesuchus not only shares a similar size but falls within the morphological disparity observed for a immature *Aetosauroides*. Based in body size and age estimation for *Aetosauroides* specimens (*sensu* Cerda & Desojo 2011, Taborda et al. 2013, 2015, Cerda et al. 2018, this study), and now for *Polesinesuchus,* we consider the variations between both two taxa to be ontogenetic. There is an apparent trend of the pit lateral to the neural spine, the infradiapophyseal laminae and the lateral fossa at the centra to become more conspicuous in individuals larger than one meter in *Aetosauroides* (Table I), a size where it is assumed to have achieved sexual maturity (see Taborda et al. 2013, 2015). As *Polesinesuchus* is found in coeval outcrop and cannot be anatomically differentiated from a immature or small individual of *Aetosauroides* we propose it as a junior synonym of *Aetosauroides scagliai*.

Based on our current understanding of *Aetosauroides* specimens found in Brazil and Argentina, the variable axial features become more marked with size increase and age, representing an ontogenetic trajectory (Fig. 17). However, this recognition does not support the synonymity of *Aetosauroides scagliai* with *Stagonolepis robertsoni* (as proposed by Lucas & Heckert 2001, Heckert & Lucas 2002b) or with the co-occurring species *Aetobarbakinoides*. Although sharing the pit lateral to the neural spine, we agree that *Aetobarbakinoides* is a valid-taxon based on the absence of the well-rimmed lateral fossa, the absence of marked infradiapophyseal laminae (mainly the posterior one) and the presence of 'U-shaped' intrapostzygapophyseal lamina, the first two expected to be present in mature *Aetosauroides*.

Roberto-da-Silva et al. (2014) have provided a detailed description of '*Polesinesuchus*' type material, which is now the best source for a juvenile *Aetosauroides* and overall immature aetosaur morphology. The majority of divergent characters used in the combined diagnostic features purported by Roberto-da-Silva et al. (2014) for the taxonomic distinction nature of '*Polesinesuchus*' is now, based on our study of new specimens from Brazil, recognized as to be shared with *Aetosauroides* (see item 6 of the Supplementary Material for further discussion). Only two of the differences pointed by Roberto-da-Silva et al. (2014) remains: the anteroposteriorly expanded medial portion of the scapula and the anterior process of the iliac blade remain as distinct characters states, which may also vary with ontogeny and need further verification. Nevertheless, another strong argument in favor of the synonymy is that '*Polesinesuchus*' shares a laterally divergent elongated postzygapophysis (extending till the mid-length of the subsequent vertebrae) with *Aetosauroides*. The ratio between the length of the postzygapophysis and the width between their tips are lower than 0.75 (Desojo & Ezcurra 2011), being present in UFSM 11070 (0.24 to 0.56) and MCP-3450-PV (0.36 to 0.50), but also in '*Polesinesuchus*' (0.38). This ratio is considered an autapomorphy of *Aetosauroides* and it is also present in '*Polesinesuchus*' type material.

Implications for aetosaur phylogeny

The re-evaluation of the type material of '*Polesinesuchus*' as an immature *Aetosauroides* specimen is an important step in our

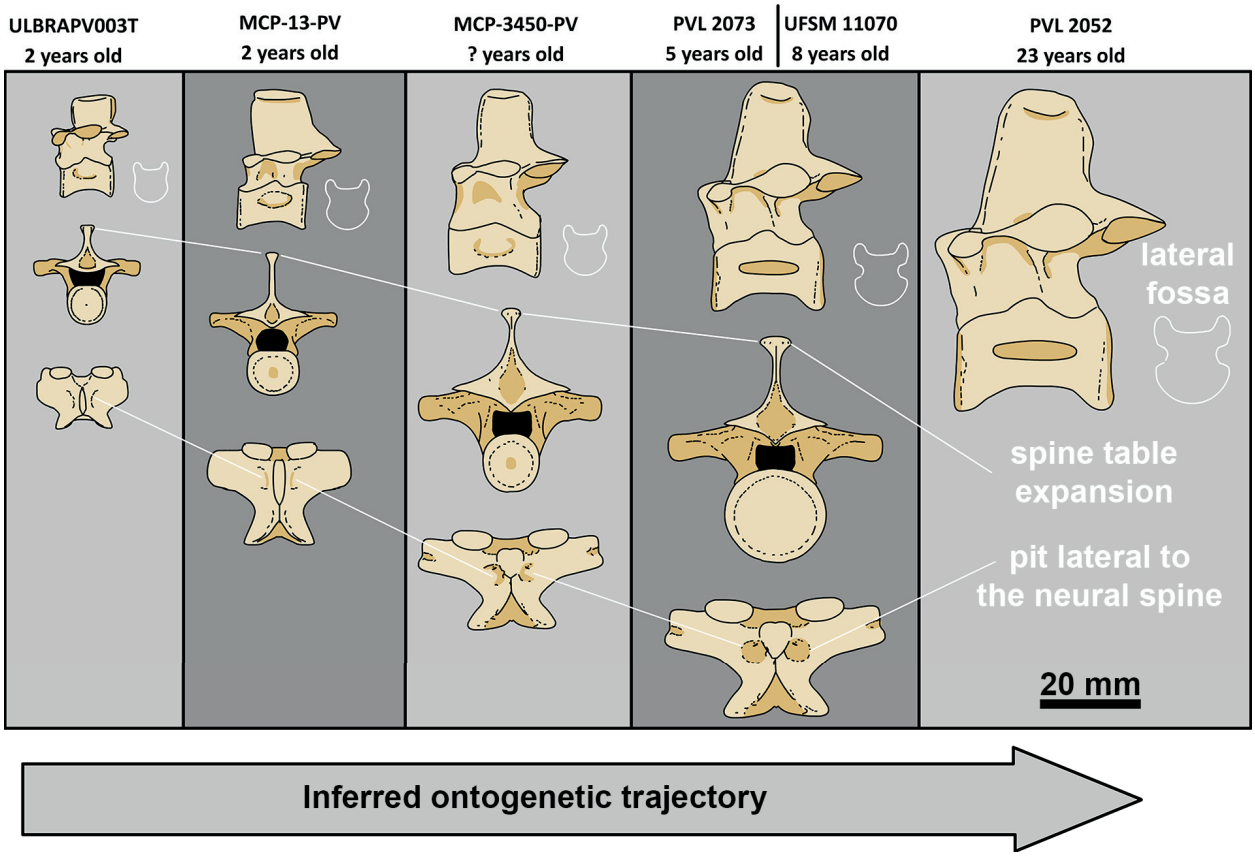

Figure 17. Ontogenetic trajectory of trunk vertebrae of *Aetosauroides*. Interpretative drawings of the three main ontogenetic changes of *Aetosauroides* trunk vertebrae: lateral fossae (white line drawing reveal the centrum cross-section); spine table expansion in anterior view; and the pit lateral to the neural spine, in dorsal view. The specimens do not necessarily preserve vertebrae with homologous regions in the trunk series, being the neural arch morphology of MCP-34050 based in an anterior trunk vertebra. The PVL 2052 drawing refers only to the centrum length, as little information is available in the posterior trunk vertebrae of that specimen. Specimens ages based on this study, Cerda & Desojo (2011) and Cerda et al. (2018).

knowledge concerning early pseudosuchian ontogenetic trends. It follows recent studies which have indicated that some small-sized aetosaurs are based mostly on immature individuals, like *Aetosaurus* (Scheyer et al. 2014, Schoch & Desojo 2016) and *Coahomasuchus chathamensis* (Hoffman et al. 2019). As indicated by Hoffman et al. (2019), this may be the same situation for other "small-sized" aetosaurs, such as *Coahomasuchus kahleorum*, *Stegomus*, and *Stenomyti*. However, some line of evidence supports the existence of some 'dwarf' aetosaurs, like the case of *Sierritasuchus* (Parker et al. 2008), *Neoaetosauroides* (e.g. Desojo & Báez 2005, Taborda et al. 2013) and *Aetobarbakinoides* (e.g. Taborda et al. 2013) as they are represented by less or nearly two-meter-long mature specimens. Recently, Marsh et al. (2020) provided evidence that the small-sized *Acaenasuchus* was neither an immature stage of the aetosaur *Desmatosuchus spurensis* (e.g. Heckert & Lucas 2002a) nor it is an aetosaur at all, representing a new clade with the enigmatic *Euscolosuchus* described by Sues (1992).

The immature based taxa '*Polesinesuchus aurelioi*' (as determined by the present study),

Aetosaurus ferratus (see Taborda et al. 2013, Schoch & Desojo 2016), and *C. chathamensis* (see Hoffman et al. 2019) were used in previous aetosaur and archosaur phylogenetic analysis (e.g. Nesbitt 2011, Desojo et al. 2012, Parker 2016a, Brust et al. 2018, Hoffman et al. 2018). Although not intended by previous researchers, the usage of terminal taxa based solely on immature specimens, without character semaphoront differentiation, may compromise the resulting tree topologies by the influence of heterochronic processes (e.g. Parsons & Parsons 2015, Sharma et al. 2017). Also, several known characters recognized here as ontogenetically variable for *Aetosauroides* are broadly used in current aetosaur and archosaur phylogenetic matrices (e.g. the deep subcircular pit lateral to neural spine, infradiapophyseal lamina and their correspondent fossae and the well-rimmed lateral fossae of the trunk vertebrae centra), demanding careful review on other pseudosuchians (Schoch & Desojo 2016, Parker 2016a, Ezcurra 2016, Ezcurra et al. 2017, Brust et al. 2018, Hoffman et al. 2018, Nesbitt et al. 2018). As indicated by Sharma et al. (2017), since ontogenetic changes are still poorly understood within early archosaurs, we hope future analysis to address discussions on the ontogenetic stage of the specimens and evaluated characters in order to improve a total evidence approach on reconstructing the phylogenetic relationships.

CONCLUSIONS

The present contribution has shown ontogenetically variable features for the trunk vertebrae of an association of four *Aetosauroides scagliai* specimens, like: (i) the increase in development of the deep pocket pit lateral to the base of the neural spine; (ii) the centrodiapophyseal laminae; and (iii) the lateral fossae ventral to the neurocentral suture. We have also demonstrated that the morphotype of '*Polesinesuchus*' falls within the intraspecific variation known to immature *Aetosauroides* specimens. Its type material now represents one of the most immature known aetosaur specimens, providing *Aetosauroides* as the best known example of an almost complete early pseudosuchian growth series. Our results decrease the known taxonomic diversity of Carnian aetosaurs in South America, restricting to two valid taxa: *Aetosauroides*, with a broad interbasinal occurrence; and *Aetobarbakinoides*, thus far endemic to Brazil. We also stressed that, as with '*Polesinesuchus*', other small-sized aetosaur species may represent juvenile ontogenetic stages rather than distinct taxa, and that the usage of this small-sized aetosaurs in phylogenetic studies, coded as representatives of the mature morphology, can contradict cladistic assumptions and generate poorly supported results.

Acknowledgements

V.D.P.N. is supported by a PhD Conselho Nacional de Desenvolvimento Científico e Tecnológico (CNPq) grant (140449/2016-7), a scholarship of Coordenação de Aperfeiçoamento de Pessoal de Nível Superior (CAPES, PDSE - 88881.187108/2018-01), a Deutscher Akademischer Austauschdienst Short-term grant (2017) and a Doris and Samuel Welles Research Fund grant (2018). J.B.D. was supported by a PICT 2018-0717 and A. Humboldt Foundation. CNPq supported A.A.S.D.R. (313494/2018-5), M.B.S (307938/2019-0) and C.L.S. (307711/2017-0). FAPERJ supported M.B.S (E-26/010.002178/2019). We are grateful to Sérgio F. Cabreira (ULBRA) and Marco Brandalise (PUCRS) for access on the studied specimens. We thank Caio Scartezini de Araújo and Luciano Dória L. de Oliveira Behle for the mechanical preparation of the UFSM 11070 specimen. We thank A. Augustin and M. Vianna for the usage of the microtomographer at the LASEPE of Pontifícia Universidade Católica do Rio Grande do Sul. Lucio Roberto-da-Silva, Eliseu Dias (Universidade Estadual do Oeste do Paraná), Adam Marsh (PEFO), Pedro H. Fonseca (UFRGS), Bianca Mastrantonio (UFRGS), Marcel Lacerda (UFRGS), Agustin G. Martinelli

(MACN), Dawid Dróżdż (ZPAL AbIII), Thiago Carlisbino (UFRGS) and Heitor Francischini (UFRGS) have made important contributions to early drafts of this paper. We thank the comments and suggestions made by the reviewers Christopher Griffin and William Parker which improved the quality of this research. We thank Adam Rountrey (UMMP), Bill Mueller (TTUP), Chris Sagebiel (TMM), Chris Mejia (UCMP), Christian Kammerer (NCSM), Daniel Brinkman (YPM), Dawid Dróżdż (ZPAL AbIII), David Gillette (MNA), Janet Gillette (MNA), Jessica Cundiff (MCZ), Kenneth Bader (TMM), Mateusz Tałanda (ZPAL AbIII), Mateusz Wosik (NMMNH), Nicole Ridgwell (NMMNH), Gabriela Cisterna (PULR), Pablo Ortiz (PVL), Patricia Holroyd (UCMP), Rainer Schoch (SMNS), Ricardo Martinez (PVSJ), Rodrigo González (PVL), Sankar Chatherjee (TTUP), Spencer Lucas (NMMNH), Stig Walsh (NMS), Tomasz Sulej (ZPAL AbIII) and William Parker (PEFO) for access to comparative specimens.

REFERENCES

BRUST ACB, DESOJO JB, SCHULTZ CL, PAES-NETO VD & DA-ROSA AAS. 2018. Osteology of the first skull of *Aetosauroides* Casamiquela 1960 (Archosauria: Aetosauria) from the Upper Triassic of southern Brazil (*Hyperodapedon* Assemblage Zone) and its phylogenetic importance. PLoS ONE 13(8): e0201450.

BROCHU CA. 1992. Late-stage ontogenetic changes in the postcranium of crocodylians. J Vertebr Paleontol 6: 209-214.

BROCHU CA. 1996. Closure of neurocentral sutures during crocodilian ontogeny: implications for maturity assessment in fossil archosaurs. J Vertebr Paleontol 16(1): 49-62.

BUTLER RJ, BARRETT PM & GOWER DJ. 2012. Reassessment of the Evidence for Postcranial Skeletal Pneumaticity in Triassic Archosaurs, and the Early Evolution of the Avian Respiratory System. PLoS ONE 7(3): e34094.

CASAMIQUELA RM. 1960. Noticia preliminar sobre dos nuevos estagonolepoideos Argentinos. Amenghiniana 2: 3-9.

CASAMIQUELA RM. 1961. Dos nuevos estagonolopoideos Argentinos (de Ischigualasto, San Juan). Rev Asoc Geol Argent 16: 143-203.

CASAMIQUELA RM. 1967. Materiales adicionales y reinterpretación de *A. scagliai* (de Ischigualasto, San Juan). Rev Mus La Plata (nueva serie), Tomo 5, Sección Paleontología 33: 173-196.

CASE EC. 1922. New reptiles and stegocephalians from the Upper Triassic of western Texas. Carnegie Instit. Wash. Washington, D.C. The Carnegie Institution of Washington 321: 1-84.

CERDA IA & DESOJO JB. 2011. Dermal armour histology of aetosaurs (Archosauria: Pseudosuchia), from the Upper Triassic of Argentina and Brazil. Lethaia 44(4): 417-428.

CERDA IA, DESOJO JB & SCHEYER TM. 2018. Novel data on aetosaur (Archosauria, Pseudosuchia) osteoderm microanatomy and histology: palaeobiological implications. Palaeontology 61: 721-745.

CHINSAMY A & RAATH MA. 1992. Preparation of fossil bone for histological examination. Palaeontol Afr 29: 39-44.

DA-ROSA ÁAS. 2004. Sítios fossilíferos de Santa Maria, RS. Ciência & Natura 26: 75-90.

DA-ROSA ÁAS. 2015. Geological context of the dinosauriform-bearing outcrops from the Triassic of Southern Brazil. J S Am Earth Sci 61: 108-119.

DA-ROSA ÁAS & LEAL LA. 2002. New elements of an armored archosaur from the Middle to Late Triassic, Santa Maria Formation, South of Brazil. Arch Mus Nac 60(3): 149-154.

DESOJO JB. 2005. Los Aetosaurios (Amniota, Diapsida) de America del Sur: sus relaciones y aportes a la biogeografia y bioestratigrafia del Triasico continental. PhD thesis, Universidad de Buenos Aires Facultad de Ciencias Exactas y Naturales, Buenos Aires, Argentina, 176 p.

DESOJO JB & BÁEZ AM. 2005. The postcranial skeleton of *Neoaetosauroides* (Archosauria: Aetosauria) from the Upper Triassic of west-central Argentina. Ameghiniana 42(1).

DESOJO JB & EZCURRA MD. 2011. A reappraisal of the taxonomic status of *A.* (Archosauria, Aetosauria) specimens from the Late Triassic of South America and their proposed synonymy with *Stagonolepis*. J Vertebr Paleontol 31(3): 596-609.

DESOJO JB, EZCURRA MD & KISCHLAT EE. 2012. A new aetosaur genus (Archosauria: Pseudosuchia) from the early Late Triassic of southern Brazil. Zootaxa 3166: 1-33.

DESOJO JB, HECKERT AB, MARTZ JW, PARKER WG, SCHOCH RR, SMALL BJ & SULEJ T. 2013. Aetosauria: a clade of armoured pseudosuchians from the Upper Triassic continental beds. In: Nesbitt SJ, Desojo JB & Irmis RB (Eds), Anatomy, Phylogeny and Palaeobiology of Early Archosaurs and their Kin, Geological Society, London, Special Publications. 379. Bath: Geological Society Publishing House, p. 275-302.

DESOJO JB ET AL. 2020. The Late Triassic Ischigualasto Formation at Cerro Las Lajas (La Rioja, Argentina): fossil tetrapods, high-resolution chronostratigraphy, and faunal correlations. Sci Rep 10: 12782.

EZCURRA MD. 2016. The phylogenetic relationships of basal archosauromorphs, with an emphasis on the systematics of proterosuchian archosauriforms. PeerJ 4: e1778.

EZCURRA MD & BUTLER RJ. 2015. Post-hatchling cranial ontogeny in the Early Triassic diapsid reptile *Proterosuchus fergusi*. J Anat 226(5): 387-402.

EZCURRA MD ET AL. 2017. Deep faunistic turnovers preceded the rise of dinosaurs in southwestern Pangaea. Nature Ecol Evol 1: 1477-1483.

FEDOROV A ET AL. 2012. 3D Slicer as an Image Computing Platform for the Quantitative Imaging Network. Magn Reson Imaging 30(9): 1323-1341.

FRANCILLON-VIEILLOT H, DE BUFFRÉNIL V, CASTANET J, GÉRAUDIE J, MEUNIER FJ, SIRE JY, ZYLBERBERG L & DE RICQLÈS A. 1990. Microstructure and mineralization of vertebrate skeletal tissues. Skeletal biomineralization: patterns, processes and evolutionary trends, p. 471-530.

GARCIA MS, PRETTO FA, DIAS-DA-SILVA S & MÜLLER RT. 2019. A dinosaur ilium from the Late Triassic of Brazil with comments on key-character supporting Saturnaliinae. An Acad Bras Cienc 91: e20180614. https://doi.org/10.1590/0001-3765201920180614.

GRIFFIN CT, STOCKER MR, COLLEARY C, STEFANIC CM, LESSNER EJ, RIEGLER M, FORMOSO K, KOELLER K & NESBITT SJ. 2020. Assessing ontogenetic maturity in extinct saurian reptiles. Biol Rev 96(2): 470-525.

GOWER DJ & SCHOCH RR. 2009. Postcranial Anatomy of the Rauisuchian Archosaur *Batrachotomus kupferzellensis*. J Vertebr Paleontol 29(1): 103-122.

HECKERT AB & LUCAS SG. 1999. New Aetosaur (Reptilia: Archosauria) from the Upper Triassic of Texas and the Phylogeny of Aetosaurs. J Vertebr Paleontol 19(1): 50-68.

HECKERT AB & LUCAS SG. 2002a. *Acaenasuchus geoffreyi* (Archosauria: Aetosauria) from the Upper Triassic Chinle Group: juvenile of *Desmatosuchus haplocerus*. Bull N M Mus Nat Hist Sci 21: 205-214.

HECKERT AB & LUCAS SG. 2002b. South American occurrances of the Adamanian (Late Triassic: latest Carnian) index taxon *Stagonolepis* (Archosauria: Aetosauria) and their biochronological significance. J Paleonto 76(5): 852-8631.

HECKERT AB, LUCAS SG, RINEHART LF, CELESKEY MD, SPIELMANN JA & HUNT AP. 2010. Articulated skeletons of the aetosaur *Typothorax coccinarum* Cope (Archosauria: Stagonolepididae) from the Upper Triassic Bull Canyon Formation (Revueltian: early-mid Norian), eastern New Mexico, USA. J Vertebr Paleontol 30(3): 619-642.

HECKERT AB, FRASER NC & SCHNEIDER VP. 2017. A new species of *Coahomasuchus* (Archosauria, Aetosauria) from the Upper Triassic Pekin Formation, Deep River Basin, North Carolina. J Paleonto 91(1): 162-178.

HOFFMAN DK, HECKERT AB & ZANNO LE. 2018. Under the armor: X-ray computed tomographic reconstruction of the internal skeleton of *Coahomasuchus chathamensis* (Archosauria: Aetosauria) from the Upper Triassic of North Carolina, USA, and a phylogenetic analysis of Aetosauria. PeerJ 6: e4368.

HOFFMAN DK, HECKERT AB & ZANNO LE. 2019. Disparate growth strategies within Aetosauria: novel histologic data from the aetosaur *Coahomasuchus chathamensis*. Anat Rec (Hoboken) 302(9): 1504-1515.

HORN BLD, MELO TM, SCHULTZ CL, PHILIPP RP, KLOSS HP & GOLDBERG K. 2014. A new third-order sequence stratigraphic framework applied to the Triassic of the Paraná Basin, Rio Grande do Sul, Brazil, based on structural, stratigraphic and paleontological data. J S Am Earth Sci 55: 123-132.

IRMIS RB. 2007. Axial skeleton ontogeny in the Parasuchia (Archosauria: Pseudosuchia) and its implications for ontogenetic determination in archosaurs. J Vertebr Paleontol 27(2): 350-361.

IKEJIRI T. 2012. Histology-based morphology of the neurocentral synchondrosis in *Alligator mississippiensis* (Archosauria, Crocodylia). Anat Rec (Hoboken) 295(1): 18-31.

LANGER MC, RIBEIRO AM, SCHULTZ CL & FERIGOLO J. 2007. The continental tetrapod-bearing Triassic of south Brazil. In: Lucas SG & Spielmann JA (Eds), The Global Triassic. Bull N M Mus Nat Hist Sci 41: 201-218.

LANGER MC, RAMEZANI L & DA ROSA AAS. 2018. U-Pb age constraints on dinosaur rise from south Brazil. Gondwana Res 57: 133-140.

LUCAS SG & HECKERT AB. 2001. The aetosaur *Stagonolepis* from the Upper Triassic of Brazil and its biochronological significance. Neues Jahrb Geol Paläontol Monatsh 2001: 719-732.

MARTINEZ RN, APALDETTI C, ALCOBER OA, COLOMBI CE, SERENO PC, FERNANDEZ E, MALNIS PS, CORREA GA & ABELIN D. 2012. Vertebrate succession in the Ischigualasto Formation. J Vertebr Paleontol 32(1): 10-30.

MARTZ J. 2002. The morphology and ontogeny of *Typothorax coccinarum* (Archosauria, Stagonolepididae) from the Upper Triassic of the American Southwest. Unpublished thesis, Texas Tech University, Lubbock, TX.

MARTZ J & SMALL BJ. 2006. *Tecovasuchus chatterjeei*, a new aetosaur (Archosauria: Stagonolepididae) from the Tecovas Formation (Carnian, Upper Triassic) Of Texas. J Vertebr Paleontol 26(2): 308-320.

MARSH AD, SMITH ME, PARKER WG, IRMIS RB & KLIGMAN BT. 2020. Skeletal anatomy of *Acaenasuchusgeoffreyi* Long and Murry 1996 (Archosauria: Pseudosuchia) and its implications for the origin of the aetosaurian carapace. J Vertebr Paleontol: e1794885.

NESBITT S. 2007. The anatomy of *Effigia okeeffeae* (ARCHOSAURIA, SUCHIA), theropod-like convergence, and the distribution of related taxa. Bull Am Mus Nat Hist 302: 1-84.

NESBITT SJ. 2011. The Early Evolution of Archosaurs: Relationships and the Origin of Major Clades. Bull Am Mus Nat Hist 352: 1-292.

NESBITT SJ, STOCKER MR, PARKER WG, WOOD TA, SIDOR CA & ANGIELCZYK KD. 2018. The braincase and endocast of *Parringtonia gracilis*, a Middle Triassic suchian (Archosaur: Pseudosuchia). J Vertebr Paleontol 37(sup1): 122-141.

O'CONNOR PM. 2006. Postcranial pneumaticity: an evaluation of soft-tissue influences on the postcranial skeleton and the reconstruction of pulmonary anatomy in archosaurs. J Morphol 267: 1199-1226.

O'LEARY MA & KAUFMAN SG. 2012. MorphoBank 3.0: Web application for morphological phylogenetics and taxonomy. http://www.morphobank.org.

PARKER WG. 2008. Description of new material of the aetosaur *Desmatosuchus spurensis* (Archosauria: Suchia) from the Chinle Formation of Arizona and a revision of the genus *Desmatosuchus*. PaleoBios New Series 28: 28-40.

PARKER WG. 2016a. Revised phylogenetic analysis of the Aetosauria (Archosauria: Pseudosuchia); assessing the effects of incongruent morphological character sets. PeerJ 4: e1583.

PARKER WG. 2016b. Osteology of the Late Triassic aetosaur *Scutarx deltatylus* (Archosauria: Pseudosuchia). PeerJ 4: e2411.

PARKER WG. 2018a. Redescription of *Calyptosuchus* (*Stagonolepis*) *wellesi* (Archosauria: Pseudosuchia: Aetosauria) from the Late Triassic of the Southwestern United States with a discussion of genera in vertebrate paleontology. PeerJ 6: e4291.

PARKER WG. 2018b. Anatomical notes and discussion of the first described aetosaur *Stagonolepis robertsoni* (Archosauria: Suchia) from the Upper Triassic of Europe, and the use of plesiomorphies in aetosaur biochronology. PeerJ 6: e5455.

PARKER WG, STOCKER MR & IRMIS RB. 2008. A new desmatosuchine aetosaur (Archosauria: Suchia) from the Upper Triassic Tecovas Formation (Dockum Group) of Texas. J Vertebr Paleontol 28(3): 692-701.

PARSONS WL & PARSONS KM. 2015. Morphological Variations within the Ontogeny of *Deinonychus antirrhopus* (Theropoda, Dromaeosauridae). PLoS ONE 10(4): e0121476.

ROBERTO-DA-SILVA LC, DESOJO JB, CABREIRA SRF, AIRES ASS, MÜLLER RT, PACHECO CP & DIAS-DA-SILVA SR. 2014. A new aetosaur from the Upper Triassic of the Santa Maria Formation, southern Brazil. Zootaxa 3764: 240-278.

SALGADO L & POWELL JE. 2010. Reassessment of the vertebral laminae in some South American titanosaurian sauropods. J Vertebr Paleontol 30(6): 1760-1772.

SCHEYER TM, DESOJO JB & CERDA IA. 2014. Bone histology of phytosaur, aetosaur, and other archosauriform osteoderms (Eureptilia: Archosauromorpha). Anat Rec 297(2): 240-260.

SCHOCH RR. 2007. Osteology of the small archosaur *Aetosaurus* from the Upper Triassic of Germany. Neues Jahrb Geol P-A 246:1-35.

SCHOCH RR & DESOJO JB. 2016. Cranial anatomy of the aetosaur *Paratypothorax andressorum* Long & Ballew, 1985, from the Upper Triassic of Germany and its bearing on aetosaur phylogeny. Neues Jahrb Geol P-A 279(1): 73-95.

SCHULTZ CL, MARTINELLI AG, SOARES MB, PINHEIRO FL, KERBER L, HORN BL, PRETTO FP, MÜLLER RT & MELO TP. 2020. Triassic faunal successions of the Paraná Basin, southern Brazil. J S Am Earth Sci 104: 102846.

SHARMA PP, CLOUSE RM & WHEELER WC. 2017. Hennig's semaphoront concept and the use of ontogenetic stages in phylogenetic reconstruction. Cladistics 33(1): 93-108.

SMALL BJ & MARTZ JW. 2013. A new basal aetosaur from the Upper Triassic Chinle Formation of the Eagle Basin, Colorado, USA. In: Nesbitt SJ, Desojo JB & Irmis RB (Eds), Anatomy, Phylogeny and Palaeobiology of Early Archosaurs and their Kin, Geological Society, London, Special Publications. 379. Bath: Geological Society Publishing House, p. 393-412.

STEFANIC CM & NESBITT SJ. 2018. The axial skeleton of *Poposaurus langstoni* (Pseudosuchia: Poposauroidea) and its implications for accessory intervertebral articulation evolution in pseudosuchian archosaurs. PeerJ 6: e4235.

STEFANIC CM & NESBITT SJ. 2019. The evolution and role of the hyposphene-hypantrum articulation in Archosauria: phylogeny, size and/or mechanics? R Soc Open Sci 6(10): 190258.

SUES HD. 1992. A remarkable new armored archosaur from the Upper Triassic of Virginia. J Vertebr Paleontol 12(2): 142-149.

TABORDA JRA, CERDA IA & DESOJO JB. 2013. Growth curve of *Aetosauroides* Casamiquela 1960 (Pseudosuchia: Aetosauria) inferred from osteoderm histology. In: Nesbitt SJ, Desojo JB & Irmis RB (Eds), Anatomy, Phylogeny and Palaeobiology of Early Archosaurs and their Kin, Geological Society, London, Special Publications. 379. Bath: The Geological Society Publishing House, p. 413-424.

TABORDA JRA, HECKERT AB & DESOJO JB. 2015. Intraspecific variation in *Aetosauroides* Casamiquela (Archosauria: Aetosauria) from the Upper Triassic of Argentina and Brazil: an example of sexual dimorphism? Ameghiniana 52(2): 173-187.

WALKER AD. 1961. Triassic Reptiles from the Elgin Area: *Stagonolepis*, *Dasygnathus* and Their Allies, Philos T R Soc B 244: 103-204.

WEDEL MJ. 2003. The evolution of vertebral pneumaticity in sauropod dinosaurs. J Vertebr Paleontol 23(2): 344-357.

SUPPLEMENTARY MATERIAL

Supplementary Appendix.

Figure S1. Standard measurements provided in Supplementary Tables.
Figure S2. Mounted blocks and the different aetosaur individuals and at least one of the *Hyperodapedon* specimens of the Faixa Nova Association.
Figure S3. Graphic plot of femur circumference (FC) and centra length (CL) for *Aetosauroides* from Brazil (UFSM 11070 and UFSM 11505) and Argentina (PVL 2073 and PVL 2052), *Polesinesuchus aurelioi* (ULBRAPV003T) and *Aetobarbakinoides brasiliensis* (CPEZ 168).
Figure S4. Atlas of *A. scagliai* (MCN-PV 2347 and MCP-3450-PV). Left atlas neural arch and atlas intercentrum of MCN-PV 2347 in (A) anterior and (B) lateral view. The atlas neural arch of MCN-PV 2347 in medial view (C). The atlas intercentrum of MCP-3450-PV in lateral (D), ventral (E) and dorsal (F) views. Abbreviations: aas, anterior articular surface; a.ic, articulation with the atlas intercentrum; ai, axis intercentrum; b.p, broken lateral projection; epi, epipophysis; fo, foramen; ic, atlas intercentrum; lfo, lateral fossa; mc, medullary cavity; na, neural arch; ; prez, prezygapophysis.
Figure S5. Ribs of *A. scagliai* (MCN-PV 2347 and UFSM 11070). a, cervical ribs of MCN-PV 2347 in posteromedial view; b, transverse cross-section of two trunk ribs of MCP-3450-PV, near the proximal end; c, proximal end of the trunk rib of UFSM 11070. Abbreviations: ca, capitulum; tu, tuberculum; vs, ventral strut.
POZW, postzygapophysis width. Numbers in italic are imprecise.
Table SI. List of comparative taxa used in this study. Bold specimens reffer to type-specimens.

Table SII. Measurements of cervical vertebrae of *Aetosauroides scagliai* (As) specimens, '*Polesinesuchus aurelioi*' (Pa) and *Aetobarbakinoides brasiliensis* (Ab). ACH, height of the anterior articular surface of the centrum; ACW, width of the anterior articular surface of the centrum; CH, centrum mean height; CL, centrum length; PCH, height of the posterior articular surface of the centrum; PCW, width of the anterior articular surface of the centrum; TVH, total vertebrae length; NAML, neural arch length; NATH, neural arch height; NSH, neural spine height; PREZW, prezygapophysis width; SPTL, spine table lenght. Numbers in italic are imprecise.

Table SIII. Proportions of cervical vertebrae measurements of analyzed *Aetosauroides scagliai* (As) specimens, '*Polesinesuchus aurelioi*' (Pa) and *Aetobarbakinoides brasiliensis* (Ab). ACH, height of the anterior articular surface of the centrum; ACW, width of the anterior articular surface of the centrum; PCH, height of the posterior articular surface of the centrum; PCW, width of the anterior articular surface of the centrum; CH, centrum height mean; CL, centrum length; TVH, total vertebrae length; NAML, neural arch length; NATH, neural arch height; NSH, neural spine height; POZW, postzygapophysis width. Numbers in italic are imprecise. Neurocentral suture: open* partially closed** closed***.

Table SIV. Measurements of trunk vertebrae centra of *Aetosauroides scagliai* specimens, '*Polesinesuchus aurelioi*' and other aetosaurs. ACH, height of the anterior articular surface of the centrum; ACW, width of the anterior articular surface of the centrum; CH, centrum mean height; CL, centrum length; PCH, height of the posterior articular surface of the centrum; PCW,

width of the anterior articular surface of the centrum; TVH, total vertebrae length; NAML, neural arch length; NATH, neural arch height; NSH, neural spine height; POZW, postzygapophysis width. Numbers in italic are imprecise.

Table SV. Proportions of trunk vertebrae measurements of analyzed *Aetosauroides scagliai* specimens, '*Polesinesuchus aurelioi*' and *Aetobarbakinoides brasiliensis* (Ab). ACH, height of the anterior articular surface of the centrum; ACW, width of the anterior articular surface of the centrum; CH, centrum mean height; CL, centrum length; PCH, height of the posterior articular surface of the centrum; PCW, width of the anterior articular surface of the centrum; TVH, total vertebrae length; NAML, neural arch length; NATH, neural arch height; NSH, neural spine height; POZW, postzygapophysis width. Numbers in italic are imprecise.

Table SVI. Measurements of sacral and caudal vertebrae of *Aetosauroides scagliai* (As), '*Polesinesuchus aurelioi*' (Po) and *Aetobarbakinoides brasiliensis* (Ab). ACH, height of the anterior articular surface of the centrum; ACW, width of the anterior articular surface of the centrum; CH, centrum mean height; CL, centrum length; PCH, height of the posterior articular surface of the centrum; PCW, width of the anterior articular surface of the centrum; TVH, total vertebrae length; NAML, neural arch length; NATH, neural arch height; NSH, neural spine height; POZW, postzygapophysis width; SPTL, spine-table lenght; SPTW, spine table width. Numbers in italic are imprecise.

Table SVII. Proportions of sacral and caudal vertebrae measurements of analyzed *Aetosauroides scagliai* (As), '*Polesinesuchus aurelioi*' (Po) and *Aetobarbabkinoides brasiliensis* (Ab). ACH, height of the anterior articular surface of the centrum; ACW, width of the anterior articular surface of the centrum; CH, centrum mean height; CL, centrum length; PCH, height of the posterior articular surface of the centrum; PCW, width of the anterior articular surface of the centrum; TVH, total vertebrae length; NAML, neural arch length; NATH, neural arch height; POZW, postzygapophysis width. Numbers in italic are imprecise. Neurocentral suture: open* partially closed closed***.**

How to cite

PAES-NETO VD, DESOJO JB, BRUST ACB, SCHULTZ CL, DA-ROSA ÁAS & SOARES MB. 2021. Intraspecific variation in the axial skeleton of *Aetosauroides scagliai* (Archosauria: Aetosauria) and its implications for the aetosaur diversity of the Late Triassic of Brazil. An Acad Bras Cienc 93: e20201239. DOI 10.1590/0001-3765202120201239.

Manuscript received on August 7, 2020;
accepted for publication on March 25, 2021

VOLTAIRE D. PAES-NETO[1]
https://orcid.org/0000-0002-6903-8504

JULIA BRENDA DESOJO[2]
https://orcid.org/0000-0002-2739-3276

ANA CAROLINA B. BRUST[1]
https://orcid.org/0000-0001-7762-1284

CESAR LEANDRO SCHULTZ[3]
https://orcid.org/0000-0001-7121-0409

ÁTILA AUGUSTO S. DA-ROSA[4]
https://orcid.org/0000-0003-4074-0794

MARINA B. SOARES[5]
https://orcid.org/0000-0002-8393-2406

[1]Universidade Federal do Rio Grande do Sul, Programa de Pós-Graduação em Geociências, Av. Bento Gonçalves 9500, 91509-900 Porto Alegre, RS, Brazil

[2]Consejo Nacional de Investigaciones Científicas y Tecnológicas (CONICET), Museo de La Plata, División Paleontología Vertebrados, Paseo del Bosque, s/n, La Plata, B1900FWA, Buenos Aires, Argentina

[3]Universidade Federal do Rio Grande do Sul, Departamento de Paleontologia e Estratigrafia, Instituto de Geociências, Av. Bento Gonçalves, 9500, 91509-900 Porto Alegre, RS, Brazil

[4]Universidade Federal de Santa Maria, Laboratório de Estratigrafia e Paleobiologia, Departamento de Geociências, Avenida Roraima, 1000, Prédio 17, Sala 1131B, 97105-900 Santa Maria, RS, Brazil

[5]Universidade Federal do Rio de Janeiro, Departamento de Geologia e Paleontologia, Museu Nacional, Quinta da Boa Vista, s/n, São Cristovão, 20940-040 Rio de Janeiro, RJ, Brazil

Correspondence to: **Voltaire Dutra Paes Neto**
E-mail: voltairearts@gmail.com

Author contributions

VDPN, JBD and MBS conceived the research. The osteological description was carried by VDPN, JBD, ACBB and MBS and the thin section was made by VDPN, JBD and by MBS. Discussions of the results were conducted by VDPN, JBD, MBS, ACBB, ASDR and CLS.

CC BY